QUANTIFYING UNCERTAINTIES AND RISKS ASSOCIATED WITH HYDROMETEROLOGICAL VARIABLES FOR BULK ELECTRIC POWER SYSTEMS AND MARKET PARTICIPANTS

Yufei Su

A dissertation submitted to the faculty at the University of North Carolina at Chapel Hill in partial fulfillment of the requirement for the degree of Doctor of Philosophy in the Department of Environmental Sciences and Engineering in the Gillings School of Global Public Health.

Chapel Hill
2020

Approved by:

Gregory Characklis

Jordan Kern

Patrick Reed

Marc Serre

Jason West

ABSTRACT

Yufei Su: Quantifying Uncertainties and Risks Associated with Hydrometerological Variables for Bulk Electric Power Systems and Market Participants.
(Under the direction of Greg Characklis and Jordan Kern)

The electrical power industry is changing rapidly. From the deregulation of power markets to the rapid increase of renewable energy penetration, over the past decade power systems have witnessed major shifts in technology, regulation and policy. These rapid transitions make the use of historical performance data a fundamentally unreliable approach to evaluate reliability and financial risks for industry participants, including utilities. This is especially true with respect to performance risks stemming from uncertainty in hydrometeorological conditions (e.g., temperature, precipitation, wind, solar irradiance), which is itself difficult to characterize due to relatively short historical records. Hydrometeorological conditions are known to influence the operations of bulk electric power systems and wholesale markets for electricity, creating a source of risk for system participants. Streamflow is the "fuel" for hydropower generation, wind speeds and solar irradiance dictate the availability of wind and solar power production, and air temperatures strongly affect heating and cooling demands. Yet, despite growing concern about the vulnerability of power systems to hydrometeorological uncertainty, few studies have been able to experimentally study the full extent of the supply and financial risks that hydrometerological

factors impose on power systems. This research focuses on quantitative characterization of the physical, environmental and financial risks posed by uncertain hydrometerological variables in a major segment of the U.S. power sector. Using the U.S. West Coast bulk power system as a test bed, this dissertation first develops an open source simulation framework capable of simulating the operations of California's wholesale market under hydrometeorological uncertainty, including events outside the historical record. The second part of this dissertation uses a 1000-year stochastic simulation of the power model to probabilistically explore the market risks associated with hydrometerological variables at annual, daily and hourly timesteps. Quantification of system wide risks then enables detailed investigation of the effects of hydrometeorological risk on a major system participant. The third part of this dissertation selects the high-profile power utility Pacific Gas and Electric (PG&E) and investigates the effects of rapid retail load defection on the utility's financial exposure to hydrometerological risk. The collective results provide novel information that can contribute to the development of improved weather risk management strategies in the electric power sector.

TABLE OF CONTENTS

LIST OF TABLES

LIST OF FIGURES

CHAPTER 1: INTRODUCTION

In bulk electric power systems and wholesale markets for electricity, a number of weather-based uncertainties impact system operations on a daily basis by directly influencing electricity demand, supply availability (including hydropower and renewable energy), and even fuel prices at fossil fuel power plants (Pesch *et al.*, 2015; Eyer and Wichman, 2018; Zhou, Voisin and Fu, 2018; Turner *et al.*, 2019). Other risks, such as market and technological changes, add additional sources of uncertainty for power systems as a whole and individual grid participants, including utilities (Hemmati, Hooshmand and Khodabakhshian, 2014; Kern, Patino-Echeverri and Characklis, 2014; Denholm *et al.*, 2015a; Su *et al.*, 2019).

Yet, quantifying these risks remains an outstanding challenge, requiring a deep understanding of the physical and economic systems at work, and sufficient data to accurately assess the probability of damaging events. Ongoing technological changes in the power industry render much of the historical record of power system performance uninformative, particularly when assessing systems' exposure to hydrometeorological uncertainties. In addition to rapid increase of renewable energy, changes in policy and market structure may be altering the manner in which power system participants experience weather risk. These uncertainties create a challenging environment for decision makers in the power sector to navigate and – at the same time –introduce several analytical challenges that must be overcome to understand how uncertainties and extreme events propagate through power systems (Stoutenburg *et al.*, 2013; Denholm *et al.*, 2015b). Developing new and improved approaches for understanding the

interactions among hydrometeorological uncertainty, physical system performance, and market outcomes will help system operators and utilities make better operational decisions and long-term resource plans.

The overarching goal of this doctoral research is to characterize weather-based uncertainties in bulk power systems and wholesale markets for electricity, and understand how these uncertainties affect a range of power system participants. For the most part, the research is focused on the U.S. West Coast bulk power system, especially California. In order to better understand the complexities of how hydrometeorological uncertainty influences California's power market, I first develop a new modeling tool to simulate system behavior. Chapter 1 presents a system-based framework to simulate the power system of California and the larger West Coast region. This framework is the methodological foundation of doctoral work and serves as the primary model and simulation tool for the rest of the chapters. The model I developed is called the California and West Coast Power (CAPOW) system model. It covers most of the states of California, Oregon and Washington, including two major wholesale electricity market, the Mid-Columbia (Mid-C) market in the Pacific Northwest and the California Independent System Operator (CAISO). A major contribution of CAPOW in the power systems community is the inclusion of a comprehensive synthetic weather generator. The synthetic weather generator produces stochastic time series records of spatially distributed air temperatures, wind speeds, streamflow and solar irradiance, such that the statistical and time series characteristics of the historical record are reproduced, while also allowing for the simulation of extreme events outside recent history. The model is Python-based and all components of the model is open source under the MIT free software license.

Using CAPOW it is possible to isolate the effects of hydrometeorological uncertainty and extremes on power systems across different time scales. Hydrometeorological conditions can influence operations of bulk electric power systems and the wholesale markets for electricity in several ways. For example, streamflow is the 'fuel' for hydropower generation, wind speed and solar irradiance directly dictate the availability of wind and solar power respectively. Air temperatures strongly influence heating and cooling demands, which are major sources of electricity consumption. Chapter 2 of this dissertation explores the impacts of hydrometeorological variables on power system performance at different time scales. A 1000-year synthetic weather dataset is pushed through CAPOW and system performance is evaluated in terms of wholesale electricity prices and emissions, two metrics importance for market participants and policy developers.

After quantifying the how hydrometeorological uncertainty creates risks for the larger West Coast power system as a whole, I zoom in to one major decision maker. I investigate the evolving weather risks faced by a major incumbent power utility in California, Pacific Gas and Electric (PG&E) by coupling CPOW with a model that simulate the utility's financial operations. Chapter 3 explores PG&E's financial exposure to hydrometeorological uncertainty, particularly fluctuations in streamflow (hydropower production), air temperatures (demand), and corresponding effects on market prices. In particular, I focus on how PG&E's exposure to weather risk is interacting with longer term declines in their retail customer base, or "load defection". The cause of this decline can be attributed to a combination of regulatory mandates, retail competition, and cheaper customer owned renewable energy. Chapter 3 investigates how the sensitivity of PG&E's financial performance to hydrometeorological uncertainty is being directly impacted by the continued defection of customers. I specifically highlight impacts to the strength of the

correlations between weather variables and financial performance and, in some cases, changes in the actual direction of exposure and the types of weather events that are most harmful.

REFERENCES

Denholm, P. et al. (2015b) Overgeneration from Solar Energy in California. A Field Guide to the Duck Chart. doi: 10.2172/1226167.

Eyer, J. and Wichman, C. J. (2018) 'Does water scarcity shift the electricity generation mix toward fossil fuels? Empirical evidence from the United States', Journal of Environmental Economics and Management. Elsevier Inc., 87, pp. 224–241. doi: 10.1016/j.jeem.2017.07.002.

Hemmati, R., Hooshmand, R. A. and Khodabakhshian, A. (2014) 'Market based transmission expansion and reactive power planning with consideration of wind and load uncertainties', Renewable and Sustainable Energy Reviews. Elsevier, 29, pp. 1–10. doi: 10.1016/j.rser.2013.08.062.

Kern, J. D., Patino-Echeverri, D. and Characklis, G. W. (2014) 'An integrated reservoir-power system model for evaluating the impacts of wind integration on hydropower resources', Renewable Energy. Elsevier Ltd, 71, pp. 553–562. doi: 10.1016/j.renene.2014.06.014.

Pesch, T. et al. (2015) 'A new Markov-chain-related statistical approach for modelling synthetic wind power time series', New Journal of Physics, 17(5), p. 055001. doi: 10.1088/1367-2630/17/5/055001.

Stoutenburg, E. D. et al. (2013) 'Variability and uncertainty of wind power in the California electric power system'. doi: 10.1002/we.1640.

Su, Y. et al. (2019) 'An open source model for quantifying risks in bulk electric power systems from spatially and temporally correlated hydrometerological processes', Environmental Modelling and Software.

Turner, S. W. D. et al. (2019) 'Compound climate events transform electrical power shortfall risk in the Pacific Northwest', Nature Communications. Springer US, 10(1). doi: 10.1038/s41467-018-07894-4.

Zhou, T., Voisin, N. and Fu, T. (2018) 'Non-stationary hydropower generation projections constrained by environmental and electricity grid operations over the western United States', Environmental Research Letters, 13(7). doi: 10.1088/1748-9326/aad19f.

CHAPTER 2: AN OPEN SOURCE MODEL FOR QUANTIFYING RISKS IN BULK ELECTRIC POWER SYSTEMS FROM SPATICALLY AND TEMPORALLY CORRELATED HYDROMETEROLOGICAL PROCESSES [1]

2.1 INTRODUCTION

In recent years, interest has grown in exploring the effects of hydrometeorological variability, and especially extreme events, on the operations of bulk power systems (large, interconnected systems of generation, transmission and load (demand)) (Franco and Sanstad, 2008; Forster and Lilliestam, 2011; van Vliet *et al.*, 2012, 2016; Tarroja, AghaKouchak and Samuelsen, 2016; Kern and Characklis, 2017; Collins *et al.*, 2018; Staffell and Pfenninger, 2018; Voisin *et al.*, 2018; Turner *et al.*, 2019). Both droughts and floods compromise the operations of hydroelectric dams (Tarroja, AghaKouchak and Samuelsen, 2016; Gleick, 2017; Su, Kern and Characklis, 2017), while droughts in particular can also impact thermal power plants that are dependent on cooling water (van Vliet *et al.*, 2012, 2016). Air temperatures influence a range of system components, most notably electricity demand for heating and cooling (Franco and Sanstad, 2008). In addition, as variable energy resources like wind and solar expand their share of the power mix, the grid is becoming more sensitive to fluctuations in wind speeds and solar irradiance (Collins *et al.*, 2018; Staffell and Pfenninger, 2018). By influencing supply and demand for electricity, hydrometeorological processes have direct impacts on pollution (e.g., increased greenhouse gas

[1] Published in *Environmental Modelling and Software*. Su, Y., Kern, Jordan D., et al. (2020) 'An open source model for quantifying risks in bulk electric power systems from spatially and temporally correlated hydrometeorological processes', *Environmental Modelling and Software*. doi: 10.1016/j.envsoft.2020.104667.

emissions (Tarroja, AghaKouchak and Samuelsen, 2016; Hardin *et al.*, 2017; Collins *et al.*, 2018)), wholesale electricity prices (Boogert and Dupont, 2005; Collins *et al.*, 2018; Seel *et al.*, 2018), and the financial standing of suppliers of electricity (e.g., retail utilities, renewable energy producers) and consumers (Boogert and Dupont, 2005; Foster, Kern and Characklis, 2015; Kern, Characklis and Foster, 2015; Kern and Characklis, 2017; Bain and Acker, 2018).

However, with few exceptions (Turner *et al.*, 2019), previous investigations fall short in assessing the holistic influence of hydrometeorological variability on bulk power systems. Past research efforts assess operational and financial risks from exposure to variability in a more limited set of hydrometeorological processes (Kern, Characklis and Foster, 2015; Collins *et al.*, 2018) (e.g., streamflow and temperatures, or wind speeds and solar irradiance;); do not consider these effects within the context of large, interconnected power systems (Kern and Characklis, 2017); and/or do not assess impacts probabilistically (Hardin *et al.*, 2017). These shortcomings may be partly attributable to the challenges of modeling bulk electric power systems at sufficient scale and resolution to simulate system operations in a realistic way, and over sufficient time horizons to explore joint uncertainty in multiple, correlated input variables.

Interconnected power systems span areas so large that system operators often have some ability to deal with spatially heterogeneous stressors. For example, a localized power supply shortfall caused by drought in one area might be managed by importing power from other areas where water, and thus electricity from hydropower production and water-cooled generators, is more abundant. From a modeling perspective, this necessitates adopting system topologies that extend beyond a single watershed, state, and region. Hydrometeorological uncertainty and power system risks can also manifest on different time scales. Extreme meteorological and hydrological conditions can have durations on the order of days (floods (Najibi and Devineni, 2017), heat

waves), weeks to months (wind "droughts"), and years (hydrological droughts (Andreadis *et al.*, 2005)), whereas power system modeling requires an hourly or sub-hourly time step (Pandzžić *et al.*, 2014). Although stochastic modeling approaches can be used to create large synthetic records of hydrometeorological processes in order to explore risks from extreme events (Reed *et al.*, 2013; Brown *et al.*, 2015), this poses a direct challenge to the use of computationally expensive integer programming within power system models (Pandzžić *et al.*, 2014), making large ensemble Monte Carlo simulations less tractable. Adding to these challenges is the potential presence of significant spatial and temporal covariance among key hydrometeorological processes (Jimenez *et al.*, 2011; Woodhouse *et al.*, 2016). If significant correlations exist, an increased number of model runs may be required to characterize the probability of coincident extremes (e.g., widespread simultaneous hydrological drought, a wind drought, and a heat wave) that may be of particular concern to power system operators (Mazdiyasni and AghaKouchak, 2015; Turner *et al.*, 2019).

The modeling scales, resolutions, and ensemble sizes required in exploring the risks to bulk electric systems from hydrometeorological variability present a challenge, and few (if any) models capable of performing this type of analysis are publically available. Given recent increased interest among the research community in modeling interconnected systems (e.g., food-energy-water (Logan, 2015)), a generalizable and open source modeling framework for simulating the influence of correlated hydrometeorological processes on power system dynamics at decision relevant scales would be a valuable addition.

The goal of this paper is to present such a framework: the newly developed California and West Coast Power (CAPOW) systems model. CAPOW was designed by the authors to explore a high profile test-bed-- the West Coast of the conterminous United States (U.S.). The bulk electric power systems covering most of the states of California, Oregon and Washington are included, as

well as the two major wholesale electricity markets active across these states (current gaps in coverage are the PacifiCorp West, Sacramento Municipal Utility District, Los Angeles Department of Water and Power balancing authorities). CAPOW is comprehensive in its treatment of stochastic weather and streamflow, simulation of relevant infrastructure (reservoir networks, power systems), and evaluation of outcomes (system costs, prices, etc.). While focused on the U.S. West Coast, the steps required in building and executing the CAPOW model (as well as much of the code) are fairly generalizable and can be transferred to other systems and interconnections of interest (Chowdhury *et al.*, 2019). Most grid specific information used in the model is publically available anywhere in the U.S. (generator size, location, fuel type, prime mover type, average heat rate, etc.). Hydrometeorological data used to simulate electricity demand, wind, solar and hydropower production are also available throughout the U.S.; as well as hourly records of renewable energy production in each balancing authority through the EIA. Analogous transmission grid information (bi-directional capacities) is publically available for all WECC areas, and for many (if not all) sub-regions in the eastern interconnection. Note that to transfer the model to other regions, additional capabilities that are not currently in CAPOW may be required (e.g., representing impacts of extreme cold, air temperatures (Henry and Pratson, 2016), and a lack of cooling water availability due to low streamflow and temperatures (van Vliet *et al.*, 2012, 2016; Miara *et al.*, 2017) on thermal power plant functionality). The model is Python-based; all code and data required to run the CAPOW model, as well as some documentation of the model, is available at https://github.com/romulus97/CAPOW_PY36 under the MIT free software license.

2.2 METHODS

Our description of methods parallels the CAPOW model's work flow (Figure 1), beginning with a discussion of surface water and electric power system topologies, including key physical assets (e.g., power plants, dams/reservoirs) and their connections (i.e., water routing between

reservoirs, high voltage transmission pathways). This is followed by a description of CAPOW's unit commitment and economic dispatch (UC/ED) model, which is used to simulate actual power system operations. The methods section ends with a description of our approach for stochastically generating model inputs from historical weather and streamflow data.

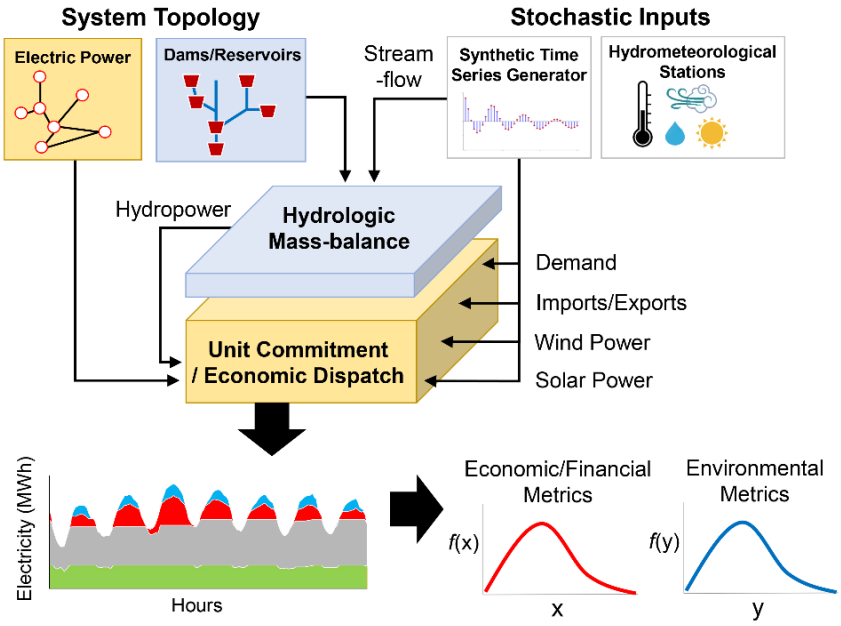

Figure 1. Model workflow. Topologies of relevant electric power and surface water infrastructure are defined first, and then synthetic time series inputs are used to drive stochastic simulation of a power system (unit commitment/economic dispatch) model. Model outputs include the least cost generation schedule, total system costs, estimated wholesale prices, and emissions.

2.2.1 System Topology

2.2.1.1Electric Power

In order to model the West Coast grid (the case study explored here), we first adopt a 21-zone topology of the Western Electricity Coordinating Council (WECC), a regulatory body charged with reducing risks to the Western grid by enforcing standards and assessing reliability (Figure 2). This topology, which has been used in the past by WECC and other researchers to assist in long term planning exercises (Mkarov *et al.*, 2010; Ho *et al.*, 2016), groups balancing authorities (utility footprints) into multiple zones that are connected via aggregated transmission pathways

throughout the region. Each zone-to-zone transmission pathway is associated with bi-directional capacities (i.e., maximum limits on zone-to-zone transfers of electricity) estimated from publically available data (Western Electricity Coordinating Council, 2016).

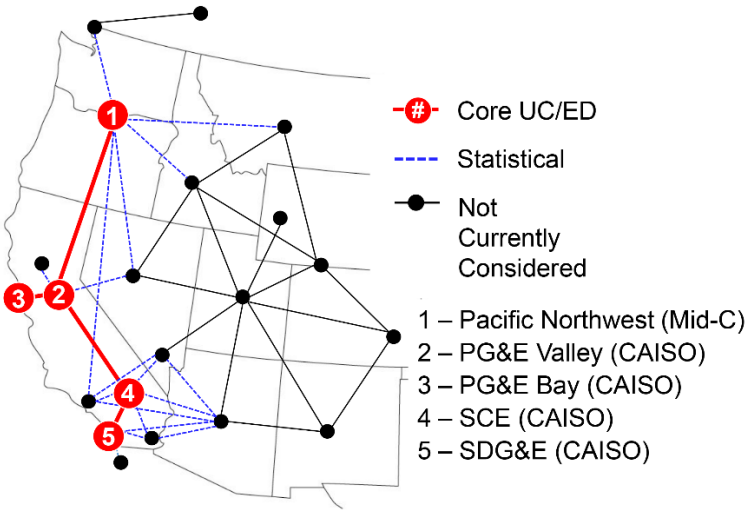

Figure 2. Power system topology used in the CAPOW modeling framework. The five red zones, comprising collections of balancing authorities (load centers and generation assets), are mechanistically modeled using unit commitment economic dispatch (UC/ED) models. Blue lines represent exchanges (imports/exports) of electricity with adjacent zones that are represented statistically. Black dots represent zones in the WECC system that are not currently represented in CAPOW.

Each zone in the network consists of: 1) the load (electricity demands) of its member balancing authorities, which fluctuate on hourly, daily, seasonal and annual time scales; and 2) a portfolio of co-located generation resources with which to meet those demands. Comprehensive databases of generators located in each node of the 21-zone WECC topology are publically available from multiple sources (U.S. EPA, 2015; Western Electricity Coordinating Council System Adequacy Planning Department, 2015). These also contain information on relevant operating characteristics for each generator (e.g., fuel type, capacity, average heat rate) that are used to formulate the UC/ED simulation model.

There are two major trading hubs for wholesale electricity on the U.S. west coast: 1) the Mid-Columbia (Mid-C) market that serves as a hub for much of the Pacific Northwest region; and

2) the California Independent System Operator (CAISO), a competitive wholesale market that manages approximately 80% of California's electricity flow. The 21-zone WECC topology shown in Figure 2 includes five nodes (red, numbered) that directly correspond to these markets: node 1 (Pacific Northwest) corresponds to the Mid-C market, and nodes 2-5 correspond to the CAISO market. Nodes 2-5 also represent the service areas of three major utilities: Pacific Gas and Electric (PG&E), Southern California Edison (SCE), and San Diego Gas and Electric (SDG&E). Currently only these five zones (and power flows among them) are modeled mechanistically using a UC/ED model. No UC/ED models exist outside these five zones. Neighboring zones are considered only in terms of their exchanges of electricity with the core UC/ED zones, and these exchanges are modeled statistically (see Supplemental Material).

2.2.1.2 Dams and Reservoirs

Recent analyses of the impacts of drought on power generation in the Western U.S. (Harto *et al.*, 2011) suggest that cooling water issues from low streamflow and high water temperatures pose a minor threat to thermal power plants in the region. Rather, the primary mechanism through which hydrologic extremes can impact power system operations is through variability in hydropower generation. Within the WECC topology shown in Figure 2, hydropower capacity makes up 58% of installed generating capacity in zone 1 (Pacific Northwest), 18% of generating capacity in zone 2 (PG&E Valley), and 4% of capacity in zone 3 (SCE) (US Environmental Protection Agency, 2018). Figure S2 in the Supplemental Material section maps major (>5MW) hydroelectric dams that participate in balancing authorities located within the five numbered zones that make up the UC/ED model. These dams primarily fall within the Columbia River Basin, which spans several Northwestern U.S. states and Canada, as well as the Sacramento River, San Joaquin River, and Tulare Lake basins in California.

Publicly available hydrologic mass balance models exist for 85% of the hydropower

capacity in the Pacific Northwest (versions of HYSSR, developed by the U.S. Army Corps of Engineers to simulate the Federal Columbia River Power System; and a ResSim model that simulates the operations of Federal dams in the Willamette River Basin). Models exist for only 12% of the hydropower capacity in California (the ORCA model (Herman and Cohen, 2019), which simulates the operations of major storage/flood control dams). In California, much of the state's hydropower capacity is privately owned and located in high altitude areas of the Sierra Nevada Mountains. Little information about the operation of these dams is publicly available, so hydropower production at these projects is simulated via an alternative approach in which hydropower production at upstream dams is predicted using observed streamflow downstream. First, for major high altitude hydroelectric dam in the Sierra Nevada Mountains, a corresponding downstream storage reservoir or stream gauge on the same river is identified. In order to predict upstream hydropower generation at a given dam using observed streamflow downstream, the calendar year is broken into four seasons: winter, spring, summer, and fall. Each season is assumed to follow a different set of "operating rules" that translate observed downstream flows into estimates of upstream hydropower production. Rules are fitted using the differential evolution algorithm in the SciPy library of Python, based on root mean squared error (RMSE) between observed and simulated hydropower production for each upstream dam.

About 15% of hydropower capacity in the Pacific Northwest and 20% of hydropower capacity in California are within the five core WECC zones that make up the UC/ED model but fall outside the four river basins mentioned above and are not associated with publicly available models. These projects are modeled by scaling hydropower generation from nearby dams. A more detailed description of how hydropower production is simulated on a daily basis can be found in the Supplemental Material.

2.2.2 Unit Commitment and Economic Dispatch Model

The power system and reservoir network topologies described above form the basis of a unit commitment/economic dispatch (UC/ED) model that we use to simulate the operation of the five numbered WECC zones in Figure 2, which include the Mid-C and CAISO markets. Simulating the UC/ED model for a single year at an hourly time step takes approximately 6 hours using the CPLEX solver on a 16-core machine with 2.5GHz processors using a Linux operating system. What follows is a general overview of the model's structure and functionality. A mathematical formulation of the UC/ED model can be found in the Supplemental Material.

We coded the UC/ED model in Python using the Pyomo mathematical optimization package, structuring it as an iterative, mixed integer linear program. Over a user-defined operating horizon (e.g., 48 hours), deterministic optimization is used to minimize the cost of meeting demand for electricity and operating reserves (including unit start costs, no load costs, fuel costs, and penalties associated with transferring electricity between zones), subject to constraints on individual generators and transmission paths. Costs are minimized by strategically "dispatching" (scheduling) generation from flexible generation resources (natural gas power plants, hydroelectric dams and system imports) on an hourly basis. Variable renewable energy (wind and solar) are not dispatchable (they can be consumed only when available); as such, they are typically treated as "electricity demand reduction" within a zone, but can be also curtailed during periods of oversupply.

A single iteration of the UC/ED model yields system costs and the least cost generating schedule over the operating horizon (e.g., hours 1-48); however, only the first 24 hours of the solution is stored. The remaining solution (hours 25-48) is discarded, and the whole process shifts one day into the future. The next iteration of the model identifies a solution for the hours 25-48, while again looking 48 hours into the future (i.e., at hours 25-72). This ensures that the model does

not have perfect foresight over unreasonably long time horizons when making decisions with path dependency (e.g., turning on baseload power plants with high "minimum up" times).

Simulation of the UC/ED model creates hourly time series outputs that track provision of electricity and operating reserves by each generator, the flow of electricity among zones, plant specific and system wide emissions of CO_2, total operating costs, and wholesale electricity prices. CO_2 emissions from each power plant are calculated using historical EPA eGrid data that are used to estimate the kg CO_2 per MWh emissions for each plant. Note that total operating costs essentially refers to the value of the objective function in each hour (the cumulative start, no load, and fuel costs across every power plant in every hour). On the other hand, wholesale electricity prices ($/MWh) are dynamic measures of the marginal value of electricity in each market, i.e., how much generators would be paid to sell their electricity in each hour. Within the optimization, wholesale prices are estimated for each zone as the shadow cost of an energy balance constraint at each zone (i.e., the change in objective function value associated with a 1MWh increase in demand at each zone). Calculating the shadow costs requires the UC/ED model to first be solved in mixed integer form, and then resolved as a linear program (keeping all binary variables fixed from the integer solution) in order to access dual values for relevant constraints in Pyomo. This yields a separate time series of wholesale electricity prices for each of the five WECC zones represented in the core UC/ED model. Prices in the Mid-C market are assumed to be equivalent to prices for the Pacific Northwest zone. To represent the CAISO market, prices for the four relevant zones in California (PG&E Valley, PG&E Bay, SCE, and SDG&E) are weighted to determine an overall price for the market, with the weights fitted via regression ($R^2 = 0.75$, $p < 1e\text{-}3$) on observed values over the period 2012-2016.

2.2.3 Stochastic Input

The primary stochastic inputs to the UC/ED model are electricity demand (hourly), wind and solar power production (hourly), and available hydropower production (daily) for each numbered zone in Figure 2. Several hydrometeorological processes (air temperatures, wind speeds, solar irradiance and streamflow) in turn drive these power system inputs. In the following section, we describe our approach for generating synthetic hydrometeorological time series.

2.2.3.1 Hydrometerological Variables

2.2.3.1.1 Air Temperature, Wind Speeds, and Solar Irradiance

We collect observed air temperatures, wind speeds, and solar irradiance data within major cities (where electricity demand is highest) and in areas known to have large amounts of installed wind and solar power capacity. Records of daily average temperature and wind speed over the period 1998-2017 come from NOAA's Global Historical Climatological Network (GHCN) for seventeen meteorological stations distributed throughout the Western U.S. (Table 1). Global horizontal irradiance data come from the National Renewable Energy Laboratory's National Solar Radiation Database (NSRDB) (Sengupta *et al.*, 2018); both "clear sky" and observed irradiance data are acquired at a 30-minute resolution and then aggregated to daily sums.

Table 1. Seventeen weather stations in the Global Historical Climatological Network and National Solar Resource Database that provide daily mean air temperature and wind speed data used in development of stochastic inputs.

Station ID	Name	Variables	Latitude	Longitude
USW00024232	SALEM AIRPORT MCNARY FIELD, OR	Wind/temps	44.90° N	123.00° W
USW00024221	EUGENE MAHLON SWEET FIELD, OR	Wind/temps	44.12° N	123.21° W
USW00024233	SEATTLE TACOMA INTERNATIONAL AIRPORT, WA	Wind/temps	47.45° N	122.30° W
USW00024131	BOISE AIR TERMINAL, ID	Wind/temps	43.56° N	116.22° W
USW00024242	PORTLAND TROUTDALE AIRPORT, OR	Wind/temps	45.54° N	122.39° W
USW00024157	SPOKANE INTERNATIONAL AIRPORT, WA	Wind/temps	47.62° N	117.53° W
USW00024163	PASCO TRI CITIES AIRPORT, WA	Wind/temps	46.26° N	119.11° W
USW00093193	FRESNO YOSEMITE INTERNATIONAL, CA	Wind/temps	36.77° N	119.71° W
USW00023230	OAKLAND METRO INTERNATIONAL AIRPORT, CA	Wind/temps	37.71° N	122.21° W
USW00023174	LOS ANGELES INTERNATIONAL AIRPORT, CA	Wind/temps	33.94° N	118.40° W
USW00023188	SAN DIEGO INTERNATIONAL AIRPORT, CA	Wind/temps	32.73° N	117.19° W
USW00023232	SACRAMENTO EXECUTIVE AIRPORT, CA	Wind/temps	38.51° N	121.49° W
USW00023293	SAN JOSE, CA	Wind/temps	37.33° N	121.88° W
USW00023234	SAN FRANCISCO INTERNATIONAL AIRPORT, CA	Wind/temps	37.62° N	122.37° W
USW00023160	TUCSON INTERNATIONAL AIRPORT, AZ	Wind/temps	32.11° N	110.93° W
USW00023183	PHOENIX AIRPORT, AZ	Wind/temps	33.43° N	112.00° W
USW00053123	LAS VEGAS AIR TERMINAL, NV	Wind/temps	36.21° N	115.19° W
NSRDB 154166	NATIONAL SOLAR RESOURCE DATABASE #1	Irradiance	40.45° N	121.66° W
NSRDB 13631	NATIONAL SOLAR RESOURCE DATABASE #2	Irradiance	38.57° N	121.7° W
NSRDB 111895	NATIONAL SOLAR RESOURCE DATABASE #3	Irradiance	36.81° N	119.38° W
NSRDB 93873	NATIONAL SOLAR RESOURCE DATABASE #4	Irradiance	35.09° N	117.3° W
NSRDB 83553	NATIONAL SOLAR RESOURCE DATABASE #5	Irradiance	34.05° N	118.38° W
NSRDB 82442	NATIONAL SOLAR RESOURCE DATABASE #6	Irradiance	33.93° N	115.9° W
NSRDB 77068	NATIONAL SOLAR RESOURCE DATABASE #7	Irradiance	33.33° N	114.7° W

Each weather station provides the data necessary to generate 365-day profiles of average temperature and wind speed for their respective locations. We use solar irradiance data to created 365-day profiles of average "clear sky" (cloudless) conditions (Figure 3).

$$TP_n = \frac{1}{Y} \sum_{y=1}^{Y} T_{n,y} \quad (1)$$

$$WP_n = \frac{1}{Y} \sum_{y=1}^{Y} WS_{n,y} \quad (2)$$

$$SP_n = \frac{1}{Y} \sum_{y=1}^{Y} S_{n,y} \quad (3)$$

Where,

TP_n = average temperature on calendar day n across Y years (℃)

$T_{n,y}$ = observed temperature on calendar day n in year y (℃)

WP_n = average wind speed on day n across Y years (m/s)

$WS_{n,y}$ = observed wind speed on day n in year y (m/s)

SP_n = average clear sky irradiance on day n across Y years (W/m^2)

$S_{n,y}$ = observed clear sky irradiance on day n in year y (W/m^2)

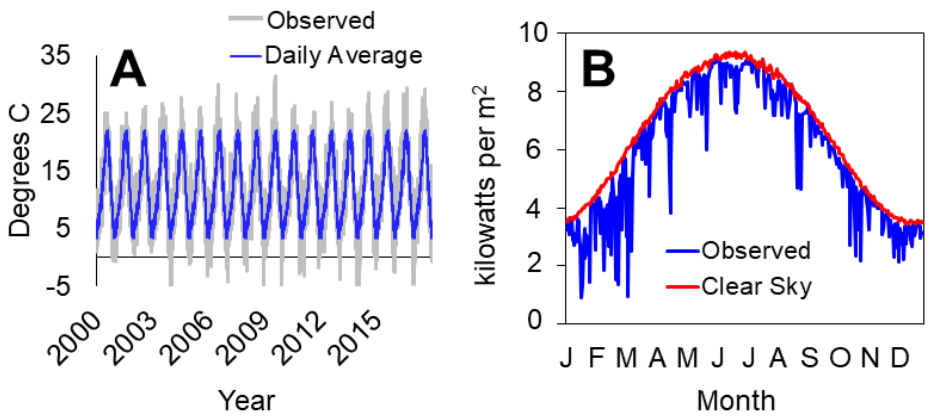

Figure 3. (A) Daily average and observed temperatures for USW00024232 (Salem, OR). (B) Daily average clear sky conditions and one year of observed irradiance for NSRDB 11895.

Synthetic values of air temperatures, wind speeds, and solar irradiance are then generated by combining these average profiles (e.g. blue series in panel A of Figure 3) with stochastic representation of the autocorrelated "residuals" that deviate from these repeating signals (e.g. the gray series in panel A of Figure 3). Average temperature and wind profiles are subtracted from observed temperature and wind speed values; this yields a daily record of zero-mean residuals (i.e., deviations from average temperature and wind speed for each calendar day over the period 1998-2017). Observed irradiance is subtracted from average clear sky irradiance, yielding a daily record of "losses" due to cloud effects.

$$RT_d = T_d - TP_n \quad (4)$$

$$RW_d = WS_d - TW_n \quad (5)$$

$$IL_d = SP_n - I_d \quad (6)$$

Where,

RT_d = residual temperature on day d (°C)

RW_d = residual wind speed on day d (m/s)

IL_d = irradiance "losses" on day d (W/m^2)

Residual temperatures and wind speeds, as well as irradiance losses, are then mean-shifted to eliminate negative values and log-transformed to approximate a Gaussian distribution. The residuals/losses for each calendar day of the year are then divided by their respective standard deviations, in order to control for seasonal heteroscedasticity.

$$WRT_d = \widehat{RT_d}/\sigma T_n \quad (7)$$

$$WRW_d = \widehat{RW_d}/\sigma W_n \quad (8)$$

$$WIL_d = \widehat{IL_d}/\sigma IL_n \quad (9)$$

Where,

WRT_d = whitened residual temperature on day d

WRW_d = whitened residual wind speed on day d

WIL_d = whitened irradiance losses on day d

$\widehat{RT_d}$ = mean shifted, log-transformed residual temperature on day d (℃)

$\widehat{RW_d}$ = mean shifted, log-transformed residual wind speed on day d (m/s)

$\widehat{IL_d}$ = mean shifted, log-transformed irradiance losses on day d (W/m^2)

σT_n = standard deviation of transformed temperature residuals on calendar day n

σW_n = standard deviation of transformed wind speed residuals on calendar day n

σIL_n = standard deviation of transformed irradiance losses on calendar day n

We then model the resultant "whitened" residuals and irradiance losses using a vector autoregressive (VAR) model, in order to capture observed covariance across variables. VAR models describe the behavior of a set of k variables over a given time period as a linear function of their past values and random samples from a multivariate normal distribution. Simulated values of each variable are stored in a $k \times 1$ vector, y_t, which has as its i^{th} element, $y_{i,t}$, the value of the i^{th} variable at time t. The "lag" of the model (i.e., the number of previous time steps that are accounted for when estimating values in y_t) is denoted by the parameter p.

$$y_t = C + A_1 y_{t-1} + A_2 y_{t-2} + \cdots + A_p y_{t-p} + \varepsilon_t \quad (10)$$

Where,

$C = k\ x\ 1$ vector of constants

$A_i = k\ x\ k$ matrix of coefficients

$\varepsilon_t = k\ x\ 1$ vector of error terms

$t =$ time period

$p =$ model lag

Simulation of y_t proceeds through random sampling of noise (ε_t) from a multivariate normal distribution with a covariance matrix estimated from whitened residuals and irradiance losses for the period 1998-2017. The number of lags considered is determined via the Akaike Information Criteria.

A fitted VAR model is used to simulate daily, whitened temperature and wind speed residuals and irradiance losses for each GHCN and NSRDB site considered, for as many years as

desired. Simulated values are then "un-whitened" by reversing Equations 7, 8, and 9 (thus restoring heteroscedasticity and non-normality); they are then added back to the 365-day profiles (reversing Equations 4, 5, and 6), yielding synthetic daily records of temperature and wind speeds.

2.2.3.1.2 Streamflow

Streamflow patterns on the west coast of the U.S. are driven by runoff from precipitation as rain and, largely, the melting of snow accumulated during the winter. Both total annual streamflow and the within year distribution of streamflow experienced in this region are known to be influenced by temperatures (Null, Viers and Mount, 2010). At the same time, there are significant correlations among the 85 separate, spatially distributed streamflow gauges that drive CAPOW's simulation of dam operations and hydropower production.

We make use of a Gaussian Copula to preserve the relationship between total annual streamflow and temperatures in stochastically generated samples. First, observed daily average temperatures (1953-2008) at the seventeen meteorological stations are converted to heating and cooling degree days, which measures deviations from 18.33 degrees C (65 degrees F).

$$HDD_{d,s} = \max(18.33 - T_{d,s}, 0) \quad (11)$$

$$CDD_{d,s} = \max(T_{d,s} - 18.33, 0) \quad (12)$$

Where,

$HDD_{d,s}$ = heating degree days on day d at station s

$CDD_{d,s}$ = cooling degree days on day d at station s

$T_{d,s}$ = average near surface air temperature on day d (℃) at station s

Total annual HDDs and CDDs are calculated, providing coarse measures of the "hotness" of a given year's summer and the "coldness" of a given year's winter. Total annual HDDs and CDDs and total annual streamflow are then transformed into quantile space by calculating the empirical cumulative probability distribution for each variable.

$$P = \mathrm{P}(Q \geq q) \tag{13}$$

Where,

Q = total annual streamflow or degree days at a given site

Empirical probabilities are transformed again into a uniform distribution ranging from -1 to 1 as follows, ensuring a mean of 0 across every variable.

$$Y = 2(P - 0.5) \tag{14}$$

The covariance matrix C across all the variables at every site is estimated, and then synthetic records of total annual streamflow and total annual HDDs and CDDs are generated by taking random samples from a multivariate normal distribution with mean 0 and covariance matrix C, then back-transforming (reversing equations 13 and 14).

The next step is to match total annual streamflow and total annual HDDs and CDDs simulated via the Copula method with the synthetic daily temperatures generated in the previous section using a vector-autoregressive (VAR) approach. Synthetic daily temperatures simulated using the VAR approach are converted to total annual HDDs and CDDs. For each year of synthetic

data desired, we select a single year of total annual HDDs and CDDs generated using the VAR approach, and then calculate the weighted average across every GHCN station. Weights are determined by the fraction of average annual flow across the 85 stream gauges that is contained within each GHCN station's surrounding area:

$$WT_s = \frac{\sum_{g=1}^{G} AVF_g}{AVT} \quad (15)$$

Where,

WT_s = weight assigned to meteorological station s

AVF_g = average annual flow at gauge site g closest to station s

AVT = average annual flow across all 85 stream gauges

The weighted total annual HDDs and CDDs from the VAR model are compared alongside pairs of weighted total annual HDDs and CDDs generated using the Copula method. The smallest mean squared error difference is identified; then the total annual streamflow values generated via the Copula method are paired with the corresponding daily temperatures (and also wind speeds and solar irradiance) generated via VAR.

Disaggregating total annual streamflow values down to a daily time step must be done in a manner that considers the potential influence of temperatures on the timing of streamflow throughout the year. For example, Figure 4 shows the relationship between winter and spring temperatures and the timing of streamflow at two major reservoirs in California. The top panel (A) shows 19 years (1997-2015) of weighted average temperatures across the GHCN stations, calculated using weights from Equation 15. Lines are colored according to the mean temperature

experienced over the first 24 weeks of the year; the dark red line indicates the year with the hottest temperatures over this period (2015), and the dark blue line indicates the year with the coolest temperatures (2010). In panels B and C, those same line colors are then used to plot contemporaneous “full natural” (unregulated) flows at Folsom Dam (panel B) and Oroville Dam (panel C) in California (two large storage dams for which there are long historical flow records). Flows are shown in terms of standardized “fractions” that are created by dividing by total annual flows at each site. At the top of panels B and C, swarm plots identify the week of maximum streamflow. For both dams, years with higher average winter and spring temperatures (red hued circles) tend to be associated with earlier peak streamflow, indicating earlier snowmelt and/or major precipitation events.

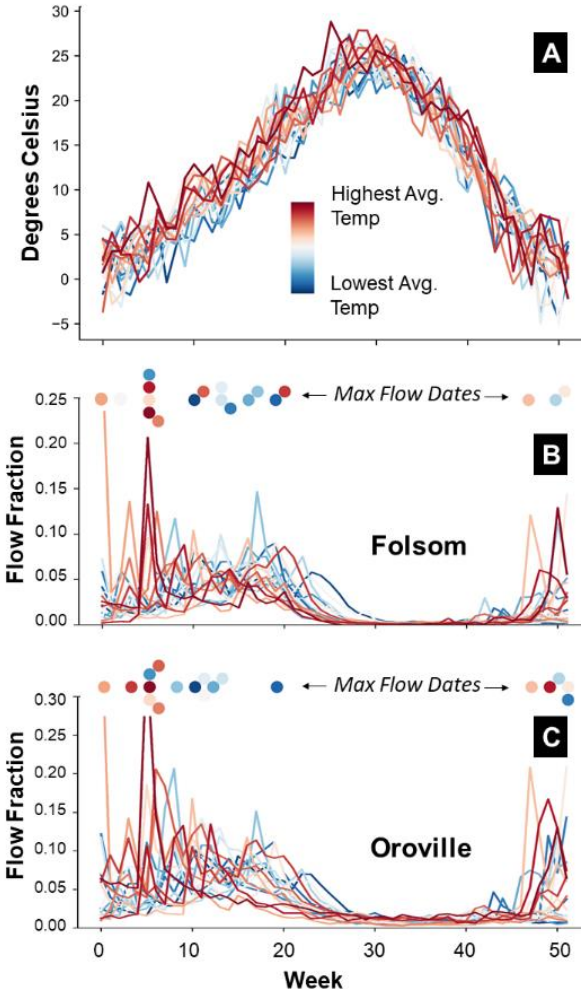

Figure 4. (A) Weighted average temperatures for the period 1997-2015, colored according to mean temperatures experienced during the first 24 weeks of the year; (B) associated unregulated daily flow fraction profiles for Folsom Dam, with a swarm plot indicating the week of maximum unregulated streamflow; (C) similar data for Oroville Dam.

In order to capture these dependencies between the timing of streamflow and temperatures, we follow a nearest neighbor clustering approach, similar to Nowak et al. (Nowak *et al.*, 2010). The weights generated in Equation 15 are used to create composite time series of temperatures across the 17 GHCN stations, for both historical and simulated temperature data. For each simulated year, the historical record is searched for a past year that exhibited the most similar winter/spring temperature profile, in terms of mean squared error. The identified historical year is then selected as the basis for determining daily flow fractions at each streamflow gauge site. For

the historical year selected, daily flow fractions are calculated as follows:

$$FF_{d,g} = \frac{DF_{d,g}}{AF_g} \quad (16)$$

Where,

$FF_{d,s}$ = flow fraction for day d at streamflow gauge site g

$DF_{d,s}$ = observed flow on day d at streamflow gauge site g

AF_g = total annual flow observed at gauge site g

Flow fractions for each gauge site are then multiplied by simulated total annual flows to yield a synthetic record of daily flows across the study area.

2.2.4 Power System Inputs

The stochastic scenario generation framework permits the exploration of large ensembles of time series for temperatures, wind speeds, solar irradiance, and streamflow. These data are then converted to associated power system inputs for the UC/ED model (time series for each zone of hourly electricity demand, wind and solar availability, daily hydropower production and imports of electricity from other areas in the Western U.S.). Table 2 provides an overview of the different approaches taken to translate raw hydrometeorological variables into power system inputs, as well as their accuracies. Multi-variate regression is used to simulate daily electricity demand, solar and wind power production, and system imports (power flows along WECC Paths listed in Table 2). Daily values are disaggregated down to an hourly time step by sampling from historical profiles. Daily values of available hydropower production are created by passing synthetic streamflow records through mass-balance hydrologic models of dams in the Columbia River basin and major

storage reservoirs in California, as well as through a machine learning representation of high altitude hydropower production in California. Detailed descriptions of all models used to translate raw hydrometeorological variables into power system inputs can be found in the Supplemental Material.

Table 2. Model results for power system inputs. R^2 values are based on daily fit for all inputs except hydropower production (weekly). In all cases, regression p-values are less than .01.

Power System Input	R^2 Value	Predictive/Independent Variables	Years
CAISO Solar Power	0.92	Irradiance	2011-2016
Pacific Northwest Wind Power	0.71	Wind speed	2011-2016
CAISO Wind Power	0.71	Wind speed	2011-2016
Pacific Northwest Electricity Demand	0.89	Temperature, wind speed, day-of-week	2010-2016
PG&E Valley Electricity Demand	0.90	Temperature, wind speed, day-of-week	2010-2016
PGE&E Bay Electricity Demand	0.79	Temperature, wind speed, day-of-week	2010-2016
SCE Electricity Demand	0.89	Temperature, wind speed, day-of-week	2010-2016
SDG&E Electricity Demand	0.80	Temperature, wind speed, day-of-week	2010-2016
WECC Path 8	0.83	Temperature, wind speed, day-of-week, Pacific Northwest hydropower	2010-2012
WECC Path 14	0.79	Temperature, wind speed, day-of-week, Pacific Northwest hydropower	2010-2012
WECC Path 3	0.63	Temperature, wind speed, day-of-week, Pacific Northwest hydropower	2010-2012
WECC Path 65	0.85	Temperature, wind speed, day-of-week, Pacific Northwest hydropower, Path 8, Path 14, Path 3	2010-2012
WECC Path 66	0.89	Temperature, wind speed, day-of-week, Pacific Northwest hydropower, Path 8, Path 14, Path 3	2010-2012
WECC Path 46	0.76	Temperature, wind speed, day-of-week, Path 65, Path 66	2010-2012
WECC Path 45	0.88	Temperature, wind speed, day-of-week, Path 46, Path 65, Path 66	2010-2012
WECC Path 24	0.84	Temperature, wind speed, day-of-week, Path 46, Path 65, Path 66	2010-2012
WECC Path 61	0.85	Temperature, wind speed, day-of-week, Path 46, Path 65, Path 66	2010-2012
WECC Path 42	0.90	Temperature, wind speed, day-of-week, Path 46, Path 65, Path 66	2010-2012
Pacific Northwest Hydropower	0.61	Streamflow	2003-2006
CAISO Hydropower	0.85	Streamflow	2001, 2005, 2010, 2011

2.3 RESULTS AND DISCUSSION

2.3.1 Validation of UC/ED Formulation

This paper proceeds with a validation of the UC/ED model's ability to reproduce observed power system dynamics (in particular, wholesale electricity prices). Wholesale prices, which are driven by changes in supply and demand, can be viewed as aggregate measures of system performance (high prices can indicate scarcity, and low prices point to abundance). We focus on an extended period of drought that occurred in California over the years 2012-2016. During this period, in-state hydropower generation decreased by an average of 40% (Gleick, 2017), forcing the state to rely significantly more on electricity from natural gas power plants. There has been considerable interest in exploring the impacts of this recent drought on pollutant emissions (Hardin *et al.*, 2017), as well as system costs and prices for retail electricity consumers (Gleick, 2017). Particularly when determining the latter, an understanding of impacts on wholesale electricity prices is necessary. Retail distribution companies in California (PG&E, SCE, and SDGE) all purchase electricity from the CAISO market. If the CAPOW model is able simulate observed wholesale electricity prices over 2012-2016 with accuracy, then the model could also be used to conduct controlled experiments designed to isolate the role of drought (and/or other hydrometorological extremes) on wholesale prices, revenues/costs for utilities, and, ultimately, retail prices for consumers. Natural gas price data used to validate the model (i.e. compare historical CAISO prices across the years 2012-2016) were obtained from EIA's natural gas hub dataset; although these data do not represent the exact price paid by power plants, they do represent dynamic prices at major gas trading hubs. These day-to-day fluctuations in gas prices are extremely important to capture. EIA's data on the delivered price of natural gas for power plants is typically listed on a monthly/annual time step, which would not allow us to capture more short term, severe price spikes.

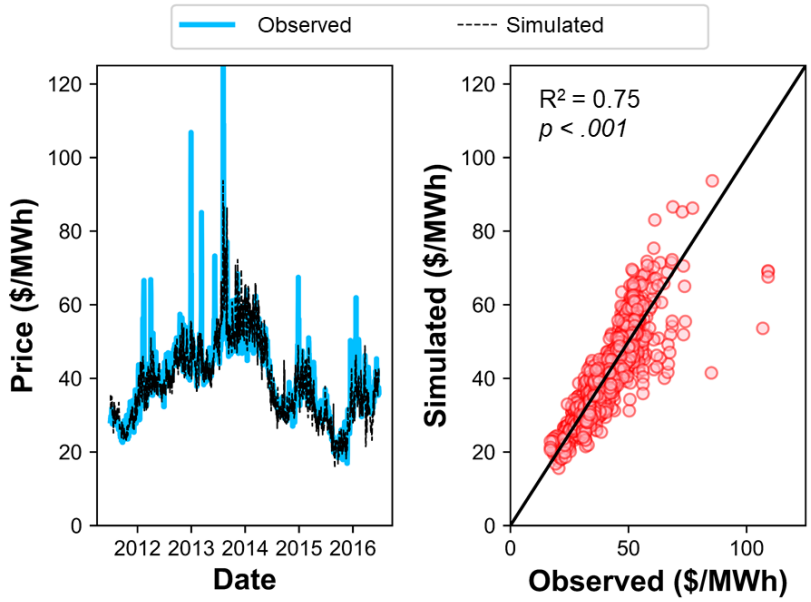

Figure 5. Daily observed vs. simulated wholesale electricity prices in the CAISO market over the period 2012-2016.

Figure 5 compares observed daily average electricity prices in the CAISO market alongside prices simulated by the UC/ED model, showing strong agreement ($R^2 = 0.75$). For the purposes of validating the UC/ED model, we used historical records of temperatures, wind speeds, solar irradiance and streamflow at the sites listed in Table 2. Thus, discrepancies between observed and simulated prices are entirely due to the UC/ED formulation itself and/or discrepancies in fuel prices experienced. In general, the model accurately captures variation in electricity prices on daily time scales and above; although model outputs include hourly prices, hourly price dynamics (e.g., "peak" and "off-peak" patterns) are not as well represented. This is expected for a model reliant on a somewhat abstracted representation of the transmission network.

2.3.1.1 Validation of stochastic inputs

The UC/ED model's ability to capture more than 70% of daily variability in CAISO electricity prices suggests that coupling it with stochastic simulations of weather and hydrology would enable probabilistic assessment of a broad set of hydrometeorological risks in wholesale

electricity markets. Before using CAPOW in this manner, however, the model's underlying "stochastic engine" (i.e., the suite of approaches used to simulate weather and hydrological variables and relevant power system inputs) must be validated.

2.3.1.2 Hydrometeorological variables

Given the large geographical extent considered, as well as the highly interconnected nature of the U.S. West Coast grid, it is important that stochastically generated meteorological and hydrological inputs exhibit the same statistical dependencies as the historical record. Figure 6 shows correlation matrices calculated using historical data from the 17 GHCN stations and 7 NSRDB sites (top left), as well as historical data from the 85 stream gauges (bottom left). These are compared alongside correlation matrices calculated using 1000 years of corresponding stochastic data generated using the approaches described in section 2.3.

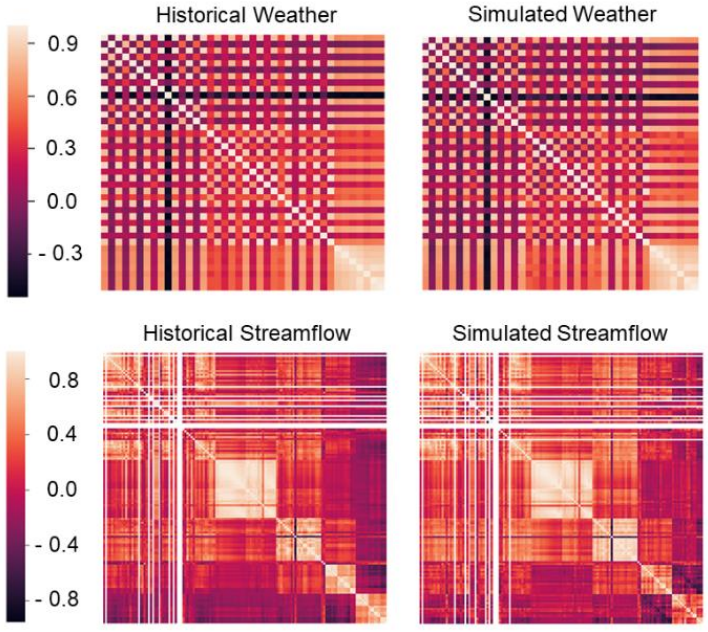

Figure 6. Historical and simulated covariance matrices for weather variables (top) across the 17 GHCN stations and streamflow (bottom) across the 85 stream gauges considered. Pockets of high values in the bottom figures indicate stream gauges within the same watershed.

Lighter areas show positive correlation (two locations/variables that are more likely to both experience high/low values simultaneously); dark areas show negative correlations. In general, results show a high degree of fidelity between historical and simulated covariance across variables and space. For example, historical and simulated streamflow correlation matrices both show the same pockets of light values, which are associated with highly correlated stream gauges located within the same watershed. Overall, these results suggest that CAPOW, when run in stochastic mode, is able to capture spatial heterogeneities in weather and hydrological processes (e.g., the likelihood of experiencing high/low temperatures/wind speeds/irradiance/streamflow simultaneously at sites distributed across the entire region).

Equally important, the underlying stochastic engine of CAPOW is able to reproduce observed statistical moments (e.g., mean, standard deviation) in hydrometeorological conditions. Figure 7 shows close agreement between historical and simulated temperatures and wind speeds across the 17 GHCN stations, in terms of percentile (1^{st}, 50^{th}, and 99^{th}), while also demonstrating the stochastic model's ability to occasionally generate more extreme min/max values than the historical record.

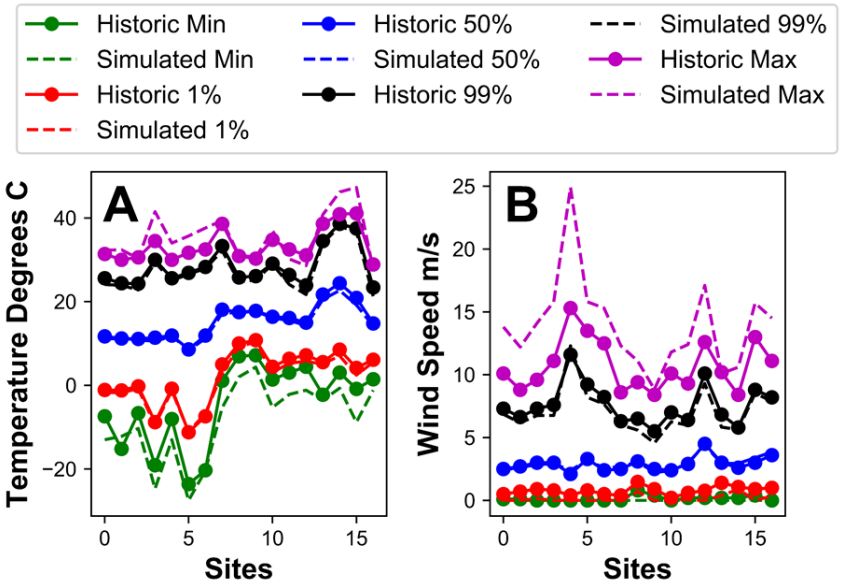

Figure 7. Historical and simulated temperatures and wind speeds across the 17 GHCN stations, distinguished by percentile (1st, 50th, and 99th) and min/max value.

In Figure 8, a similar comparison is shown using streamflow data. Each panel includes historical (blue/red circles) and simulated (black line) values for each of the 85 stream gauges considered. Red circles represent gauges in California (mostly the Sierra Nevada Mountains) and blue circles represent gauges in the Pacific Northwest (mostly the Columbia River Basin). Each panel represents a different percentile (1st/50th/99th) as well as min/max values. Note that in some cases, negative values are shown. This is an artifact of our use of BPA's modified flow dataset, which consists of historical flows at gauge sites in the Columbia River Basin with modern human withdrawals applied. At certain gauge sites, this results in negative flow values (water is subtracted from reservoir storage). In general, results suggest close agreement between the distributions of historical and stochastically generated streamflow values, while also demonstrating the stochastic model's ability to occasionally generate more extreme min/max values than the historical record.

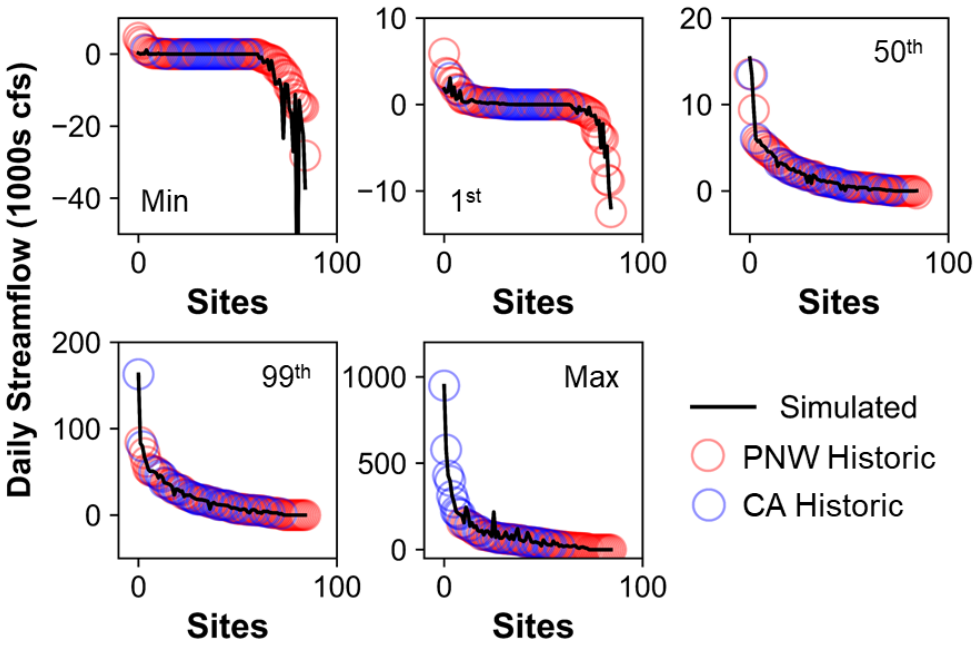

Figure 8. Historical and simulated streamflows across the 85 stream gauges considered, distinguished by percentile (1st, 50th, and 99th) and min/max values.

2.3.2 Power system inputs

A suite of models is used to translate raw temperatures, wind speeds, solar irradiance and streamflows into power system inputs, including multivariate regression (wind and solar power, electricity demand, system imports/exports) and hydrologic mass-balance operational models of reservoirs (hydropower). Coupled with our stochastic weather and streamflow generation techniques, these models yield realistic time series of power system inputs that mimic historical data on seasonal, daily and hour time scales (Table 2).

For example, Figure 9 (panel A) shows historical (blue) and simulated (red) seasonality in wind power "capacity factor" (a unitless number between 0 and 1 corresponding to the average hourly output of a wind farm as a fraction of installed capacity), aggregated for the entire CAISO system. The simulated data is produced by coupling stochastically generated wind speeds at GHCN stations with a multivariate regression model of system-wide wind power availability based

on wind speeds (Table 2), and then adding in a record of synthetic residuals (model errors). Results indicate alignment with historical data on a monthly basis, with highest capacity factors occurring in the summer and lowest during winter.

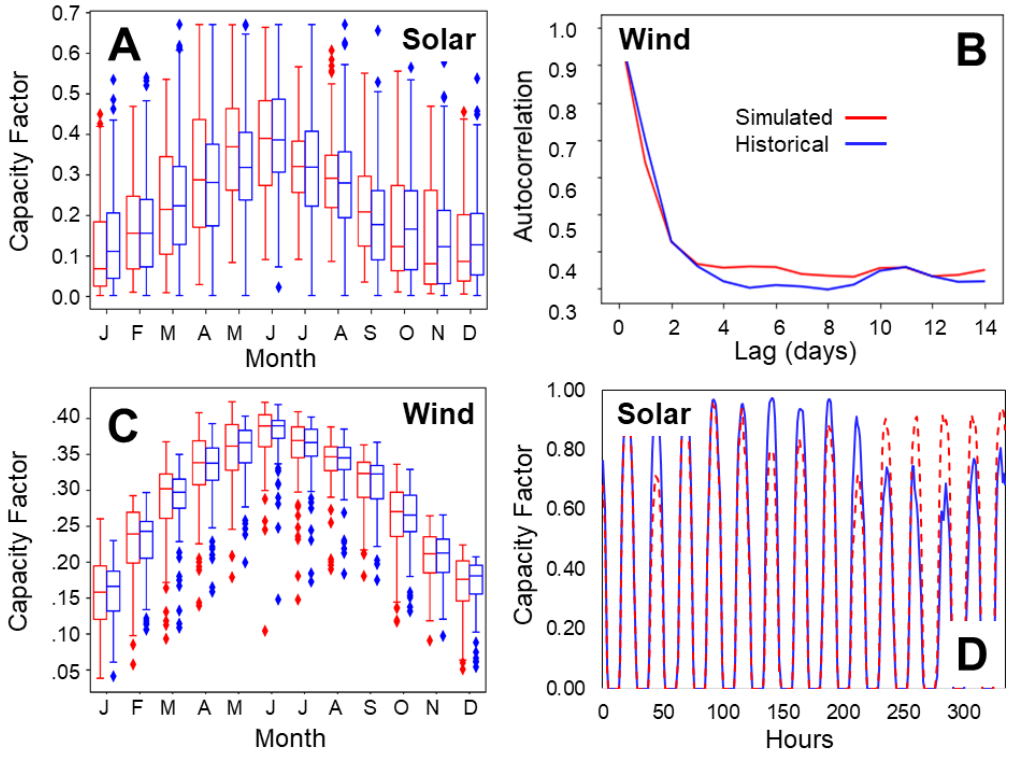

Figure 9. (A) Capacity factors for aggregate wind power production in the CAISO market; (B) daily autocorrelation in daily wind power production in the CAISO market; (C) capacity factors for aggregate solar power production in the CAISO market; (D) hourly capacity factors for a sample period in the CAISO market. Red = simulated; blue = historical.

This approach is also able to reproduce hourly and daily time series characteristics for wind power production. Figure 9 (panel B) shows close agreement between historical and simulated daily autocorrelation in wind power production, suggesting the model does an adequate job preserving any statistically significant "memory" in daily wind power production.

Figure 9 (panel C) shows historical and simulated seasonality in solar power capacity for the CAISO system. The simulated data is produced by coupling stochastically generated solar irradiance (minus cloud effects) at seven NSRDB sites with a multivariate regression model of

system-wide solar power availability based on site-specific irradiance. Results indicate alignment with historical data on a monthly basis, again with highest capacity factors occurring in the summer months and lowest during winter. This approach is also able to reproduce hourly and daily time series characteristics for solar power production. Figure 9 (panel D) compares hourly capacity factors produced using historical irradiance data for a week in Summer 2006 alongside stochastically generated solar power data for the same calendar week (with differences being due to simulated cloud effects).

Consideration was also given to volume of simulations required to achieve statistical "convergence" between historical and simulated power system inputs. A primary motivating factor in developing the underlying framework of the CAPOW model is to explore the impacts of hydrometeorological uncertainty, especially extreme events, on power systems and electricity markets. To be useful in this regard, the stochastic engine of CAPOW, as well as the UC/ED model, must be run over a sufficiently large number of years to produce the kind of low probability, high magnitude "tail" events that are concerning to grid participants (e.g., episodes of extreme shortfalls or overabundance in supply). Considering the high computational requirements of the UC/ED model, which relies on mixed integer programming, a relevant question is "how many years are enough"?

Figure 10 explores this question for the CAPOW model. Each panel shows data for a different input in the CAISO system: hydropower production, wind power production, load (electricity demand), and "net load", defined here as load minus total renewable energy (wind, solar, and hydropower) and resources considered to be "must run", like nuclear and geothermal. Net demand is an important metric because it represents the amount of electricity that would need to be met by dispatchable generators (coal and natural gas).

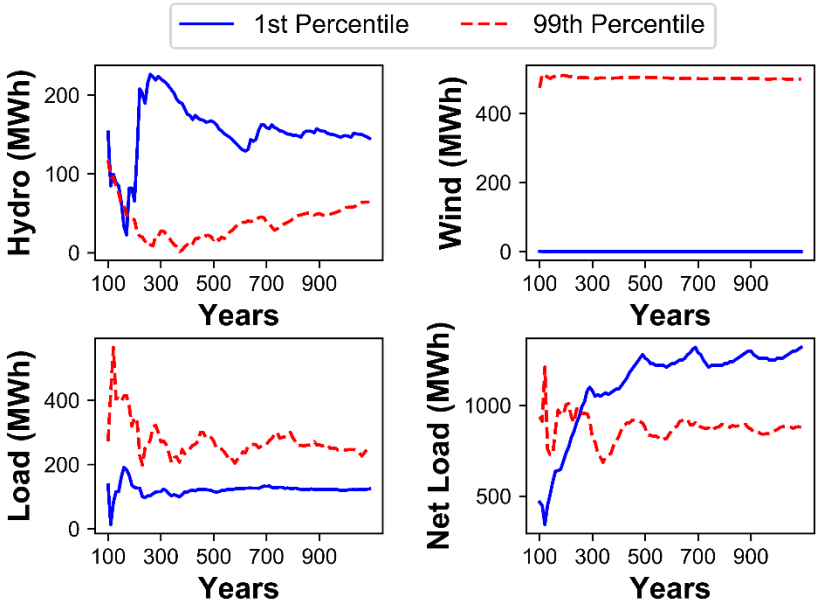

Figure 10. Absolution deviations between historical and simulated inputs to the CAISO system in terms of their 1st and 99th percentile values, tracked as a function of the volume of simulation years.

The colored lines measure the absolute difference between the historical record and synthetically generated values as a function of simulation volume. For example, in the bottom left panel (load), the red line tracks the difference between the historical record and stochastically simulated values, in terms of the 99th percentile of hourly electricity demand. At low simulation volumes, this difference starts at around 280MWh (average hourly demand in the CAISO market is more than 25,000MWh, indicating an error of less than 1%). As the number of simulated years increases, the absolute difference first increases but then stabilizes, appearing to asymptotically approach a value close to 220 MWh. Stabilization occurs when increasing the number of simulation years has a negligible impact on the difference between historical and simulated values. Figure 10 shows that simulations from CAPOW's stochastic engine tend to converge statistically after about 1000 years, suggesting this would be a reasonable lower bound on simulation volume to run through the UC/ED model.

Overall, our results suggest that CAPOW's stochastic engine is able to reproduce historical statistical characteristics across multiple hydrometeorological variables and power system inputs, needing approximately 1000 simulation years to achieve stable distributions. A final validation step is to evaluate whether the stochastic engine creates an expanded distribution of system states—in other words, does simulation over 1000 years cause extreme events outside the historical record to emerge from joint uncertainties in individual system processes? Without directly running the UC/ED model, a preliminary analysis of this kind can be conducted using net load as a metric of interest, since this typically correlates strongly with electricity prices and would be a key indicator of the potential for system shortfalls (extremely high net demand) and oversupply (extremely low net load).

Figure 11 evaluates net load in the CAISO system under different scenarios. The shaded areas show the distribution of net load over the period 1953-2008, simulated using historical hydrometeorological data. Colors correspond to different percentiles of net load (ranging from 1st to 99th) as well as the min/max values for this time period. Net load simulated using hydrometeorological data from 1953-2008 is then compared alongside actual historical net load recorded for a recent year, 2016, which is represented with a black line. For the most part, actual net load for 2016 is enveloped by the distribution of values simulated using 1953-2008 hydrometeorological data. Figure 11 also shows minimum and maximum values acquired from 1000 years of synthetic runs produced by the stochastic engine of CAPOW (blue dotted lines). Min/max values produced by the stochastic engine suggest that the CAPOW model, by exploring joint uncertainties in hydrometeorolgical variables at sufficiently high simulation values, is able to access rare extreme events outside the historical record. The additional information provided by stochastic modeling appears to be especially valuable during late summer, when net load is the

highest and the stochastic model produces maximum values that are considerably larger than the highest values simulated using weather and hydrology from 1953-2008. These more extreme synthetic values are likely to include rare but plausible "compound" events in which combinations of high electricity demand, and low renewable energy availability create extremely high net load, with associated risks for reliability and high market prices.

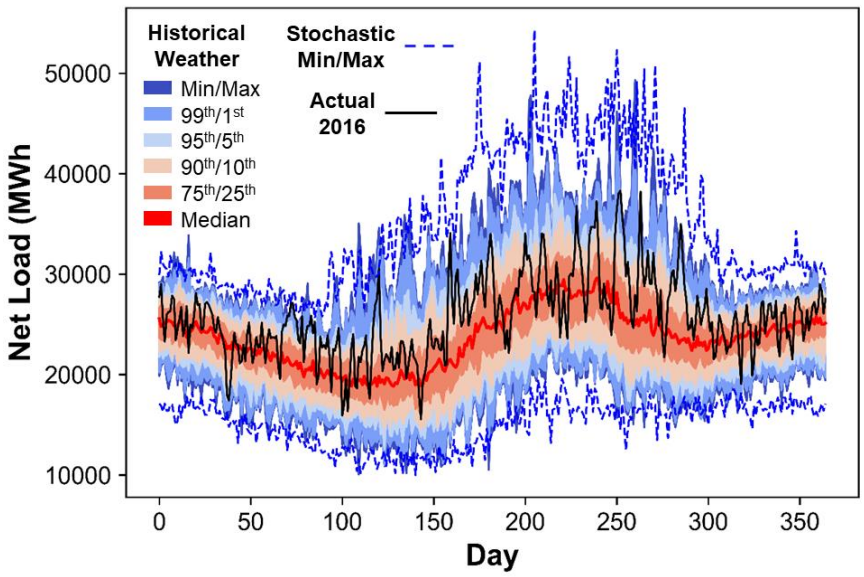

Figure 11. Simulated net demand for the California wholesale market. Shaded areas represent uncertainty driven by historical (1953-2008) hydrometeorological time series. Actual historical net demand for a single year (2016) is also shown in black. Enveloping the simulations forced by historical hydrometeorology are minimum and maximum values acquired from 1000s of synthetic runs produced by the stochastic model.

2.4 CONCLUSION

Despite growing interest in the potential vulnerabilities of bulk electric power systems to hydrometeorological variability (and extremes), there are few (if any) open source modelling packages capable of exploring this issue in a comprehensive manner. This paper presents a new model, CAPOW, which we specifically designed to explore the influence of joint uncertainties in temperatures, wind speeds, solar irradiance and streamflow on bulk power systems and wholesale electricity markets. CAPOW couples synthetic generation of hydrometeorological variables with

simulation models of relevant infrastructure (dams, power plants), allowing for in depth exploration of the role of weather and hydrology on system outcomes. The model is free and downloadable via public online repositories.

The CAPOW model uses a topological representation of the conterminous U.S. West Coast power system to form a unit commitment and economic dispatch (UC/ED) model that simulates system operations and tracks performance (system costs, prices, etc.) on an hourly basis. When using historical weather and streamflow data as inputs to the model, it is able to capture 75% of the variability in daily electricity prices in the CAISO market. Although designed specifically with the U.S. West Coast in mind, the steps taken to construct CAPOW, as well as much of the code base, can be extended to other systems of interest. However, some critical functionalities may need to be added. For example, CAPOW does not currently represent thermal power plant curtailments due to inadequate cooling water supplies caused by low streamflows and high temperatures.

When run in stochastic mode, CAPOW couples the UC/ED model with a "stochastic engine" that creates synthetic records of temperatures, wind speeds, solar irradiance and streamflow for a group of 17 meteorological stations, 7 solar resource assessment sites, and 85 stream gauges distributed throughout the West Coast. Stochastically generated hydrometeorological variables are used to predict electricity demand (via temperatures, wind speeds), wind power production (via wind speeds), solar power production (via irradiance) and hydropower availability (via streamflows), which then drive the UC/ED model. The statistical properties (moments, cross correlations, time series characteristics) of synthetic data produced mirror those of the historical record, while also allowing for the generation of more extreme (but plausible) events. Exploring the joint uncertainty in relevant hydrometeorological variables is computationally tractable, with the statistics of stochastic simulations converging with the

historical record after approximately 1000 simulation years. Overall, our framework –which is also easily transferrable across systems and geographic areas—simulates the operations of bulk electric power systems and wholesale markets at sufficient scales and resolutions to simulate system operations in a realistic way, and over sufficient time horizons to explore joint uncertainty across multiple, correlated variables of interest. As such, it should prove to be a valuable future resource for direct grid participants as well as the research community, particularly in answering questions related to the vulnerability of the grid to future changes in hydroclimate, as well as the sensitivity of variable renewable energy dominated grids to stationary hydrometeorological uncertainty.

REFERENCES

Andreadis, K. et al. (2005) 'Twentieth-Century Drought in the Conterminous United States', American Meteorological Society, 6, pp. 985–1001.

Bain, D. and Acker, T. (2018) 'Hydropower Impacts on Electrical System Production Costs in the Southwest United States', Energies, 11(2), p. 368.

Boogert, A. and Dupont, D. (2005) 'The nature of supply side effects on electricity prices: The impact of water temperature', Economics Letters, 88(1), pp. 121–125.

Brown, C. et al. (2015) 'The future of water resources systems analysis: Toward a scientific framework for sustainable water management', Water Resources Research, 51(8), pp. 6110–6124.

Chowdhury, K. et al. (2019) 'PowNet: a power systems analysis model for large-scale water-energy nexus studies', Journal of Open Software.

Collins, S. et al. (2018) 'Impacts of Inter-annual Wind and Solar Variations on the European Power System', Joule, 2(10), pp. 2076–2090.

Forster, H. and Lilliestam, J. (2011) 'Modeling thermoelectric power generation in view of climate change.', Regional Environmental Change, 4, pp. 327–338.

Foster, B., Kern, J. and Characklis, G. (2015) 'Mitigating Hydrologic Financial Risk in Hydropower Generation Using Index-based Financial Instruments', Water Resources and Economics, 10, pp. 45–67.

Franco, G. and Sanstad, A. (2008) 'Climate change and electricity demand in California', Climatic Change, 87(139).

Gleick, P. (2017) Impacts of California's Five-Year (2012-2016) Drought on Hydroelectricity Generation. Oakland, CA.

Hardin, E. et al. (2017) 'California Drought Increases CO2 Footprint of Energy Production', Sustainable Cities and Society, 28, pp. 450–452.

Harto, C. B. et al. (2011) 'Analysis of drought impacts on electricity production in the Western and Texas Interconnections of the United States', Argonne National Laboratory, p. 161. doi: 10.2172/1035461.

Henry, C. and Pratson, L. (2016) 'Effects of Environmental Temperature Change on the Efficiency of Coal- and Natural Gas-Fired Power Plants', Environmental Science and Technology, 50(17), pp. 9764–9772.

Herman, J. and Cohen, J. (2019) The Operation of Reservoirs in California (ORCA) model.

Ho, J. et al. (2016) Planning Transmission for Uncertainty: Applications and Lessons for the

Western Interconnection.

Jimenez, P. et al. (2011) 'The Effect of Heat Waves and Drought on Surface Wind Circulations in the Northeast of the Iberian Peninsula during the Summer of 2003', Journal of Climate, October.

Kern, J. and Characklis, G. (2017) 'Evaluating the Financial Vulnerability of a Major Electric Utility in the Southeastern U.S. to Drought under Climate Uncertainty and an Evolving Generation Mix', Environmental Science and Technology, 55(15), pp. 8815–8823.

Kern, J. D., Characklis, G. W. and Foster, B. T. (2015) 'Natural gas price uncertainty and the cost-effectiveness of hedging against low hydropower revenues caused by drought', Water Resources Research, 51(4), pp. 2412–2427. doi: 10.1002/2014WR016533.

Logan, B. (2015) 'Urgency at the Nexus of Food, Energy, and Water Systems', Environmental Science and Technology, 2(6), pp. 149–150.

Mazdiyasni, O. and AghaKouchak, A. (2015) 'Substantial increase in concurrent droughts and heatwaves in the United States', Proceedings of the National Academy of Sciences, 112(37), pp. 11484–11489.

Miara, A. et al. (2017) 'Climate and water resource change impacts and adaptation potential for US power supply', Nature Climate Change, 7(11), pp. 793–798.

Mkarov, Y. et al. (2010) Analysis Methodology for Balancing Authority Cooperation in High Penetration of Variable Generation.

Najibi, N. and Devineni, N. (2017) 'Recent Trends in Frequency and Duration of Global Floods', Earth System Dynamics Discussions, 9, pp. 757–783.

Nowak, K. et al. (2010) 'A nonparametric stochastic approach for multisite disaggregation of annual to daily streamflow', Water Resources Research, 46.

Null, S., Viers, J. and Mount, J. (2010) 'Hydrologic Response and Watershed Sensitivity to Climate Warming in California's Sierra Nevada', PLoS ONE, 5(4).

Pandzžić, H. et al. (2014) 'Effect of time resolution on unit commitment decisions in systems with high wind penetration', in IEEE PES General Meeting. National Harbor, MD: IEEE.

Reed, P. et al. (2013) 'Evolutionary multiobjective optimization in water resources: The past, present, and future', Advances in Water Resources, 51, pp. 438–456.

Seel, J. et al. (2018) Impacts of High Variable Renewable Energy Futures on Wholesale Electricity Prices, and on Electric-Sector Decision Making.

Sengupta, M. et al. (2018) 'The National Solar Radiation Data Base (NSRDB)', Renewable and Sustainable Energy Reviews, 89(June), pp. 51–60.

Staffell, I. and Pfenninger, S. (2018) ‘The increasing impact of weather on electricity supply and demand’, Energy, 145(15), pp. 65–78.

Su, Y., Kern, J. D. and Characklis, G. W. (2017) ‘The impact of wind power growth and hydrological uncertainty on financial losses from oversupply events in hydropower-dominated systems’, Applied Energy, 194. doi: 10.1016/j.apenergy.2017.02.067.

Tarroja, B., AghaKouchak, A. and Samuelsen, S. (2016) ‘Quantifying climate change impacts on hydropower generation and implications on electric grid greenhouse gas emissions and operation’, Energy, 111(15), pp. 295–305.

Turner, S. W. D. et al. (2019) ‘Compound climate events transform electrical power shortfall risk in the Pacific Northwest’, Nature Communications. Springer US, 10(1). doi: 10.1038/s41467-018-07894-4.

US Environmental Protection Agency (2018) Emissions and Generation Resource Integrated Database (eGRID).

van Vliet, M. et al. (2012) ‘Vulnerability of US and European electricity supply to climate change’, Nature Climate Change, 2.

van Vliet, M. et al. (2016) ‘Power-generation system vulnerability and adaptation to changes in climate and water resources’, Nature Climate Change, 6, pp. 375–380.

Voisin, N. et al. (2018) ‘Opportunities for joint water-energy management: Sensitivity of the 2010 western U.S. electricity grid operations to climate oscillations’, Bulletin of the American Meteorological Society, 99(2), pp. 299–312. doi: 10.1175/BAMS-D-16-0253.1.

Western Electricity Coordinating Council (2016) 2016 Power Supply Assessment.

Western Electricity Coordinating Council System Adequacy Planning Department (2015) Release Notes for the WECC 2024 Common Case. Salt Lake City, UT.

Woodhouse, C. et al. (2016) ‘Increasing influence of air temperature on upper Colorado River streamflow’, Geophysical Research Letters, 43, pp. 2174–2181.

CHAPTER 3: COMPOUND HYDROMETEROLOGICAL EXTREMES ACROSS MULTIPLE TIMESCALES DRIVE VOLATILITY IN CALIFORNIA ELECTRICITY MARKET PRICES AND EMISSIONS[2]

3.1 INTRODUCTION

Hydrometeorological conditions influence the operations of bulk electric power systems and wholesale markets for electricity. Streamflow is the "fuel" for hydropower generation, wind speeds and solar irradiance dictate the availability of wind and solar power production, and air temperatures affect heating and cooling demands. Despite growing concern about the vulnerability of power systems to hydrometeorological uncertainty, including "compound" extremes (multiple extremes occurring simultaneously)(Mazdiyasni and AghaKouchak, 2015; Zscheischler *et al.*, 2018), quantifying baseline probabilistic risks remains difficult even without factoring in climate change. Here, we use newly developed power system simulation software(Su *et al.*, 2020) to show how uncertainties in spatially and temporally correlated hydrometeorological processes affect market prices and greenhouse gas emissions in California's wholesale electricity market. Results highlight the need for larger synthetic datasets to access rare, yet plausible system states that have not occurred in the recent historical record. We find that time scale strongly controls which combinations of hydrometeorological variables cause extreme outcomes. Although scarcity caused by low streamflows and high air temperatures has long been considered a primary concern in Western power markets(Hardin *et al.*, 2017; Turner *et al.*, 2019), market prices are more impacted

[2] Published in *Applied Energy*. Su, Y., Kern, Jordan D, et al. (2020) 'Compound hydrometeorological extremes across multiple timescales drive volatility in California electricity market prices and emissions', *Applied Energy*. Elsevier, 276(April), p. 115541. doi: 10.1016/j.apenergy.2020.115541.

by weather and streamflow conditions that lead to an overabundance of energy.

Variability in hydrometeorological processes is known to affect electricity supply and demand(Staffell and Pfenninger, 2018), with corresponding impacts on emissions of greenhouse gases and other air pollutants, system cost(Gleick, 2016) and reliability(Van Vliet *et al.*, 2016; Voisin *et al.*, 2016, 2018; Zhou, Voisin and Fu, 2018; Turner *et al.*, 2019), and market prices(Woo *et al.*, 2017; Jordehi, 2018; Mureddu and Meyer-Ortmanns, 2018). However, limited number of extreme events are captured by historical observations of weather and streamflow, necessitating the use of large stochastic simulations to assess associated risks. Stochastic simulations can enable higher fidelity characterization of the possible combinations of extreme hydrometeorological states and rare, yet plausible, events outside recorded observations, but care must be taken to reconstruct spatial and temporal statistical dependencies among multiple hydrometeorological variables and across scales. Risk characterization must also consider the interconnected topologies of bulk electric power systems, which give system operators some ability to manage spatially explicit hydrometeorological stress(Scorah, Sopinka and van Kooten, 2012). Previous efforts to quantify the impacts of hydrometeorological extremes on large, interconnected power systems have not fully captured the joint uncertainties that occur in spatially distributed weather and streamflow processes(Harto *et al.*, 2011; Voisin *et al.*, 2016; Kern and Characklis, 2017; Turner *et al.*, 2019) or adequately explored the role of timescale in controlling which phenomena drive extreme grid outcomes. In this study, we focus on the California Independent System Operator (CAISO) system, through which 80% of California's electricity flows(CAISO, 2018). There is increased interest in the effects of drought and extreme events on the California grid(Franco and Sanstad, 2008; Stoutenburg *et al.*, 2013; Hardin *et al.*, 2017; Forrest *et al.*, 2018; Zohrabian and Sanders, 2018), but at present no study has characterized electricity price and emissions outcomes

probabilistically under hydrometerological uncertainty.

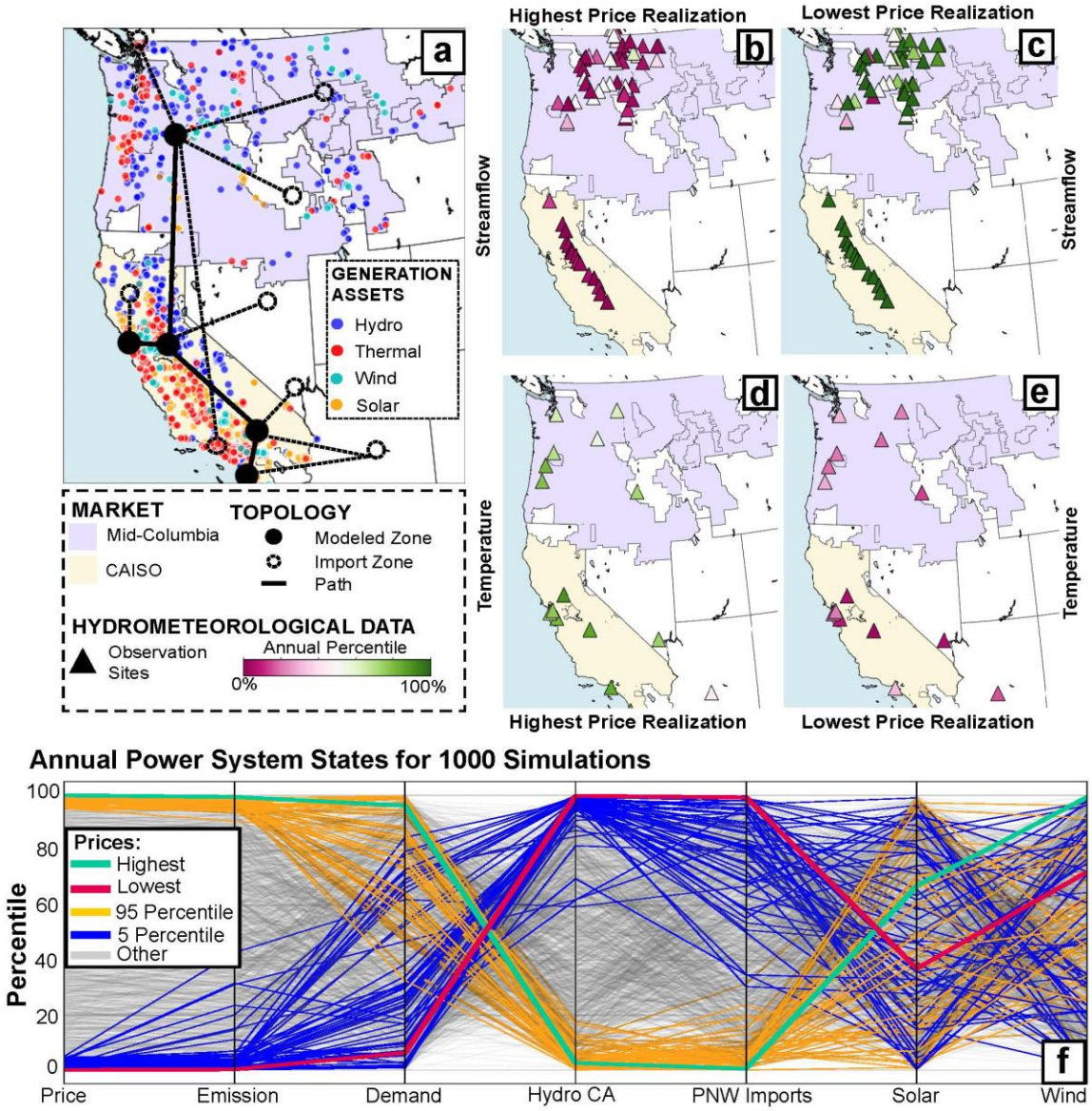

Figure 12: (a) Topology of the power system model used and map of existing generators; (b) Average temperatures (by weather station) during the highest price year; (c) Average temperatures during the lowest price year; (d) Streamflows gauge status during the highest price year; (e) Streamflows during the lowest price year; (f) Below the maps, a parallel coordinate plot of the 2 system performance metrics and 5 state variables for all 1000 simulation realizations. The highest, lowest, 5th and 95th percentiles are highlighted in color.

We employ a new open source simulation framework designed specifically to evaluate performance of the CAISO system under uncertainties in multiple spatially and temporally correlated hydrometeorological processes. The core of the model is a stochastic "engine" that

generates synthetic daily records of temperatures, wind speeds, solar irradiance and unregulated streamflow at more than 100 monitoring stations distributed throughout the West Coast. The statistical properties (moments, cross correlations, spatial and temporal structure) of the synthetic hydrometeorological data mirror those of the historical record, and the large number of synthetic records (i.e., capable of observing hundreds or thousands of replicate worlds) allows for a better characterization of plausible compound extreme events. The augmented synthetic records of hydrometeorological variables are used to simulate hourly electricity demand, wind power production, solar power production and hydropower availability. These synthetic power system inputs drive a multi-zone unit commitment and economic dispatch model that simulates the hourly operation of the West Coast bulk electric power system, including the CAISO market (Figure 12a), outputting corresponding hourly time series of power plant emissions and market prices for electricity. We quantify risks associated with compound hydrometeorological extremes by simulating system behavior over 1000 synthetic years, which previous results(Su *et al.*, 2020) suggest is a sufficient simulation length to capture uncertainty in the multivariate state space and produce higher fidelity estimates of plausible compound extreme events relative to the historical record. For comparison, we also simulated the model using historical hydrometeorological data from the years 2000-2017.

3.2 METHODS

In this study we make use of the California and West Coast Power System (CAPOW) model, an open source simulation framework for evaluating risks from correlated hydrometeorological processes in bulk power systems and wholesale electricity markets. The modeling framework is Python-based and all code and data are freely available via online public repositories.

CAPOW accurately reproduces historical price dynamics in CAISO, while also offering

unique capabilities for stochastic simulation that are well suited to the challenge of isolating the role of hydrometeorological uncertainty (including compound extreme events) on electricity market outcomes. The following sections provide details about the two core components of the model: a simulation model for relevant electric power system infrastructure, and a stochastic "engine" that generates synthetic records of hydrometeorological variables. Full mathematical descriptions of the CAPOW model's core components, as well as extensive validation, can be found in a separate paper by the authors(Su *et al.*, 2020).

3.2.1 Power Systems Model

The model's geographical scope covers nearly the entirety of the U.S. West Coast bulk electric power system (Figure 1a), including most of the states of Washington, Oregon and California and the operations of two wholesale electricity markets, the Mid-Columbia (Mid-C) market in the Pacific Northwest and the California Independent System Operator (CAISO) in California. The modeled system topology is comprised of 5 major zones (1 in the Pacific Northwest, and 4 in California), which are linked via aggregated high voltage transmission pathways. Interregional connectivity is also captured between California and the Southwest (power flows are modeled statistically). Each zone is associated with a portfolio of generating resources and a separate time series of electricity demand. We simulate power system operations using a multi-zone unit commitment and economic dispatch (UC/ED) model formulated as a mixed integer linear program. The model's objective function is to minimize the cost of meeting demand for electricity and operating reserves in the two major markets represented, and its solution is constrained by limits on individual generators, the capacity of transmission pathways linking zones, and others.

The primary inputs to the model are time series of hourly electricity demand, available

wind and solar power production in each zone, and available hydropower production on a daily basis, which the optimization program dispatches according to its least cost objectives. Measured outputs are hourly zonal electricity prices ($/MWh) and cumulative system wide emissions of CO_2 (tons). In a given hour, we estimate the market price of electricity for each zone as the shadow price of an energy balance constraint. The overall market price for CAISO is calculated using a weighted regression among prices for the four California zones, trained on historical (2012-2016) zonal price data. In this study, we assume 2016 grid resources, including thermal generators, hydroelectric dams, installed wind/solar power capacity, and high voltage transmission pathways. Power plant emissions (tracked in terms of CO_2 equivalents) are calculated on the individual generator level using the simulated generation amount (MWh) and an emission coefficient for each plant (kg/MWh) developed from the U.S. EPA eGrid(EPA, 2018) database.

3.2.2 Stochastic engine

The use of historical hydrometeorological observations to evaluate critical infrastructure performance has a long history of misrepresenting risks from extreme events(Lall and Sharma, 1996; Sahin and Sen, 2001; Herman *et al.*, 2016). This practice is particularly problematic when considering risks associated with compound events. Very long simulations may be needed to adequately explore complex joint uncertainties that exist across variables, time and space, and produce rare combinations of system states that are especially hazardous(Borgomeo, Farmer and Hall, 2015; Herman *et al.*, 2016). Thus, in this study we rely on an expanded (1000-year) synthetic dataset of relevant hydrometeorological variables and power system inputs, which is created as follows.

First, historical records of daily average temperature and wind speed data at 17 major airports (Figures 12d and 12e, Figure S1 in the Supplemental Information) across the U.S. West

Coast are gathered from the NOAA Global Historical Climatological Network(NOAA, no date). Temperature data cover the period of 1970-2017, whereas wind data only cover 1998-2017. Missing wind data (1970-1998) at each site are filled by bootstrapping historical data, conditioned on minimizing the RMSE of daily temperatures. Concurrent records of global horizontal irradiance are taken from 6 sites (Figure S1 in the Supplemental Information) in the National Renewable Energy Laboratory's National Solar Radiation Database (NSRDB)(Sengupta *et al.*, 2018). Observed daily streamflow for 108 sites (Figures 12b and 12c) throughout the Pacific Northwest and California are taken for 1954-2008 from the BPA Modified Streamflow database((BPA) Bonneville Power Administration, no date) and the California Data Exchange Center (CDEC) (CDEC, no date).

Synthetic hydrometeorological data is created in a manner that maintains the statistical moments for each individual process, as well as spatiotemporal and cross correlations among variables on multiple time scales (annual, seasonal, daily, hourly). Using the hourly historical data for temperatures and wind speeds described above, we generate an average 365-day profile for each observation site. Similarly, historical irradiance data is used to create a profile of average 'clear sky' conditions. The period 1998-2017 is selected to ensure contemporaneous records across variables. Then residuals of the temperature and wind profiles are generated by subtracting the average profile from observed data. A similar operation is done for irradiance data to calculate "losses" in irradiance from cloud coverage. All of the residuals are transformed to approximate Gaussian distributions, and then the transformed residuals are used to parameterize a vector autoregressive (VAR) model to capture both autocorrelation and covariance across variables. The error terms in the VAR model are generated from a multivariate Gaussian distribution whose covariance matrix is calculated from the historical residual dataset. The number of lags is

determined using the Akaike Information Criteria (AIC). Synthetic residuals for temperatures, wind speeds and irradiance are then "un-whitened", back-transformed and added to the average profiles to simulate daily temperature, wind speed and irradiance values.

Creating synthetic streamflow records is a two-step process. First, Gaussian Copulas are used to capture observed statistical dependences among total annual streamflow at each gauge site, and between total annual streamflow and average air temperatures. To do this, a longer observed temperature record (1953-2008) at seven meteorological stations is transformed into heating and cooling degree days (HDDs and CDDs, respectively), which are measures of deviation from 18.33 degrees Celsius (65 degrees Fahrenheit). Then total annual HDDs and CDDs are calculated by summing the daily HDDs and CDDs for each year, providing a coarse measure of each historical year's "hotness" and "coolness". Historical annual HDDs, CDDs and total annual streamflow for all sites are then transformed into quantile space by calculating empirical cumulative probability distribution of each variable:

$$P = \mathrm{P}(Q \geq q) \tag{1}$$

Where,

Q = variable of interest (total annual streamflow, annual HDDs, annual CDDs)

The empirical distribution is transformed again into a uniform distribution between -1 and 1 to ensure a zero-mean coherent dataset:

$$Y = 2(P - 0.5) \tag{2}$$

Random samples are then drawn from a multivariate Gaussian distribution with mean 0 and covariance matrix $\boldsymbol{C}$ calculated across all sites and values of HDDs, CDDs and annual streamflow. The sampled data is then transformed back by reversing equations 1 and 2.

The next step is to disaggregate total annual flows down to a daily time step. The synthetic samples of HDDs, CDDs and annual streamflow produced using the Gaussian Copula approach are matched with daily temperatures generated using the VAR model described above. For each year of synthetic data desired, a single year of HDDs and CDDs generated using the VAR model is selected via mean squared error. The corresponding daily temperatures are then compared alongside the historical record to find the year with the most similar spring and summer temperatures. Daily flow fractions for this historical year are then multiplied by total annual flows simulated via Gaussian Copula to produce a synthetic record of streamflow at each gauge site. This approach ensures that synthetic streamflow capture observed correlations across sites, as well as relationships with temperatures, on multiple time scales.

After synthetic records of hydrometeorological variables (temperatures, wind speeds, solar irradiance and streamflow) are created, these time series are translated into corresponding records of power system inputs. Using multi-variate regression models fitted to historical data, we use synthetic hydrometeorological data to create daily records of zonal electricity demand (via temperatures and wind speeds); wind power generation (via wind speeds); and solar power production (via irradiance), with regression residuals then represented using VAR processes. Hourly values are resampled from historical datasets maintained by BPA and CAISO.

Daily values of available hydropower production are created by passing synthetic streamflow records through mass-balance hydrologic models of dams in the Columbia River basin and major storage reservoirs in in California, as well as through a machine learning representation

of high altitude hydropower production in California; a small amount of remaining hydropower capacity is also represented via scaled model outputs. Daily hydropower availability is then dispatched optimally on an hourly basis by the UC/ED model. Detailed descriptions of all models used to translate raw hydrometeorological variables into power system inputs can be found in Su et al(Su *et al.*, 2020).

Synthetic records of zonal electricity demand, hydropower availability, and variable renewable energy production are then pushed through the UC/ED model, resulting in 1000-year empirical distributions of prices and emissions. In order to isolate the role of hydrometeorological uncertainty and compound extremes on system outcomes, we initially fix the price of natural gas at $4.5/MMBtu. Thus, when we refer in this paper to prices in specific historical years (e.g. 2011), this should be interpreted as prices calculated by the model using observed 2011 hydrometeorological data, assuming a natural gas price of $4.5/MMBtu.

3.3 RESULTS AND DISCUSSION

The results of this study add new insights to what is already known about the California grid's vulnerability to hydrometeorological extremes. In an average year, 15% of California's electricity demand is met by hydropower produced within the state(California Energy Commission, 2019). Moreover, additional hydropower is imported from the Pacific Northwest and Southwest, making California particularly exposed to periodic West Coast-wide drought(Wise, 2016). There is also growing evidence that climate change is increasing the likelihood that precipitation deficits in California are associated with elevated temperatures (including heat waves (Diffenbaugh, Swain and Touma, 2015; Mote *et al.*, 2016; Zscheischler and Seneviratne, 2017)),

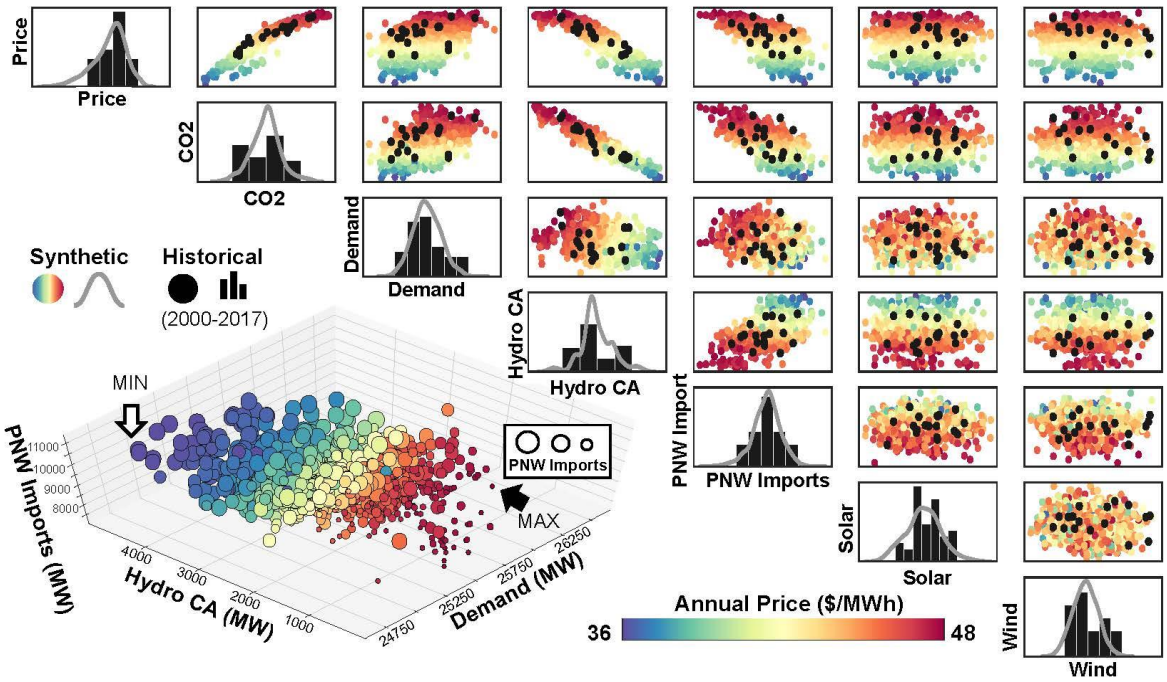

Figure 13: Above diagonal: pair plots for the two performance metrics (wholesale prices and CO2 emissions) and five system state variables. Annual values from the stochastic simulation (colored dots) are plotted alongside annual values using historical hydrometeorology (black dots). Diagonal: distributions of power system state variables and performance metrics produced using historical (black) and synthetic (gray) hydrometeorological data. Below diagonal: 3D scatter plot for demand, California hydropower and PNW imports on an annual basis. Size of the dots correlate to the value of PNW imports. The diagonal plots are the distribution for each variable using either historical or synthetic datasets. Bottom half, color coded correlation for all variables.

potentially leading to more frequent periods of low hydropower production and high electricity demand occurring simultaneously. Compound hydrometeorological extremes can also create an overabundance of energy on the California grid. As its dependence on variable renewable energy grows(California Energy Commission, 2015), California is experiencing more frequent periods of oversupply during which the available supply of renewable and must-run generation eclipses the grid's demand for electricity. A notable example occurred in early 2017, when California experienced an extreme wet period initiated by several atmospheric rivers, leading to high streamflow, an abundance of hydropower and, in combination with wind and solar, frequent negative prices and renewable energy curtailment throughout February and March (Trabish, 2017).

We have structured the discussion of our results by time scale, beginning with annual and then proceeding to seasonal, daily and hourly time steps. On an annual time scale, we find that simultaneous extremes in temperatures and streamflow occurring across the entire West Coast causes the largest swings in market prices and CO_2 emissions. We also find that extremes in emissions and prices are strongly positively correlated. The year with the highest average price ($48/MWh) out of the 1000 synthetic realizations is an extremely "hot and dry" year (see Figure 12b and 21d). High air temperatures increase demand for electricity in California, while low streamflow across the West Coast decreases the availability of hydropower in California as well as the availability of hydropower imports from the Pacific Northwest (PNW). The green line in panel Figure 12f tracks performance metrics (prices, emissions) and state variables for the same highest-price year that is depicted in Figures 12b and 12d. This connection between "hot and dry" years and high average prices is largely consistent among years with prices at or above the 95th percentile (gold lines in Figure 12f). The lowest price year ($36/MWh) is on average extremely "cool and wet" (Figure 12c and 12e). These conditions correspond to low electricity demand, plentiful hydropower in California, and abundant hydropower imports from the Pacific Northwest (red line in Figure 12f). The connection between "cool and wet" conditions and low prices is largely consistent among years that experience prices at or below the 5th percentile (blue lines in Figure 12f).

The 3D scatter plot in the lower diagonal of Figure 13 shows how CAISO prices respond to different combinations of in-state hydropower production, PNW imports, and electricity demand over the 1000-year synthetic dataset. Note that the min and max price years (the same ones shown in Figure 12) correspond to simultaneous extremes in these three state variables. The pair plots in the upper right show that the stochastic synthetic records capture historical correlations among key

state variables and performance metrics on an annual basis. Figure 13 highlights the importance of utilizing the expanded synthetic dataset to capture plausible compound extreme events that are not well represented within the limited length of the available historical record. In each plot along the diagonal, the stochastic results capture a wider range of decision relevant outcomes than what is produced by the historical data.

In particular, we find that using historical hydrometeorological data alone yields a systematic bias that underrepresents years in which the CAISO market could frequently experience "oversupply" (i.e., when available hydropower, variable renewable energy and must run resources exceed demand) and extremely low market prices. The lowest-price year from the historical dataset is 2011— a wet year with relatively cool temperatures and an average price of $41.28/MWh. That price is equivalent to the 10th percentile of the 1000-year synthetic dataset, meaning there are many plausible combinations of hydrometeorological variables that force both prices (and emissions) considerably lower than 2011 (Table 3). In contrast, recent historical hydrometeorological data provide a better approximation of extreme scarcity on the California grid, thanks in part to the state having recently experienced a very extreme historic drought during 2012-2016 (an event with an estimated return period of between 1-in-500 and 1-in-1200 years)(Griffin and Anchukaitis, 2014; Belmecheri *et al.*, 2016).

Table 3. Comparison of annual power system performance metrics and state variables among the highest and lowest price years from the 1000-year synthetic dataset and historical dataset (1970-2017).

Simulation	Price	Emissions	Demand	Hydro CA	PNW Imports	Solar	Wind
Synthetic (MAX)	99.999%	99.40%	96.30%	2.60%	0.40%	67.10%	99.30%
Synthetic (MIN)	0.001%	0.20%	6.30%	99.80%	99.20%	37.10%	71.90%
Historical (2015)	98.34%	98.26%	92.19%	2.74%	16.45%	38.12%	26.33%
Historical (2011)	10.30%	9.30%	32.56%	89.04%	83.47%	75.83%	24.09%

We also find positive correlations between hydropower availability in California and PNW imports (which consist mostly of hydropower) (upper diagonal of Figure 13), confirming a finding from previous studies(Ryu *et al.*, 2010; Pathak *et al.*, 2018) that these two regions, whose

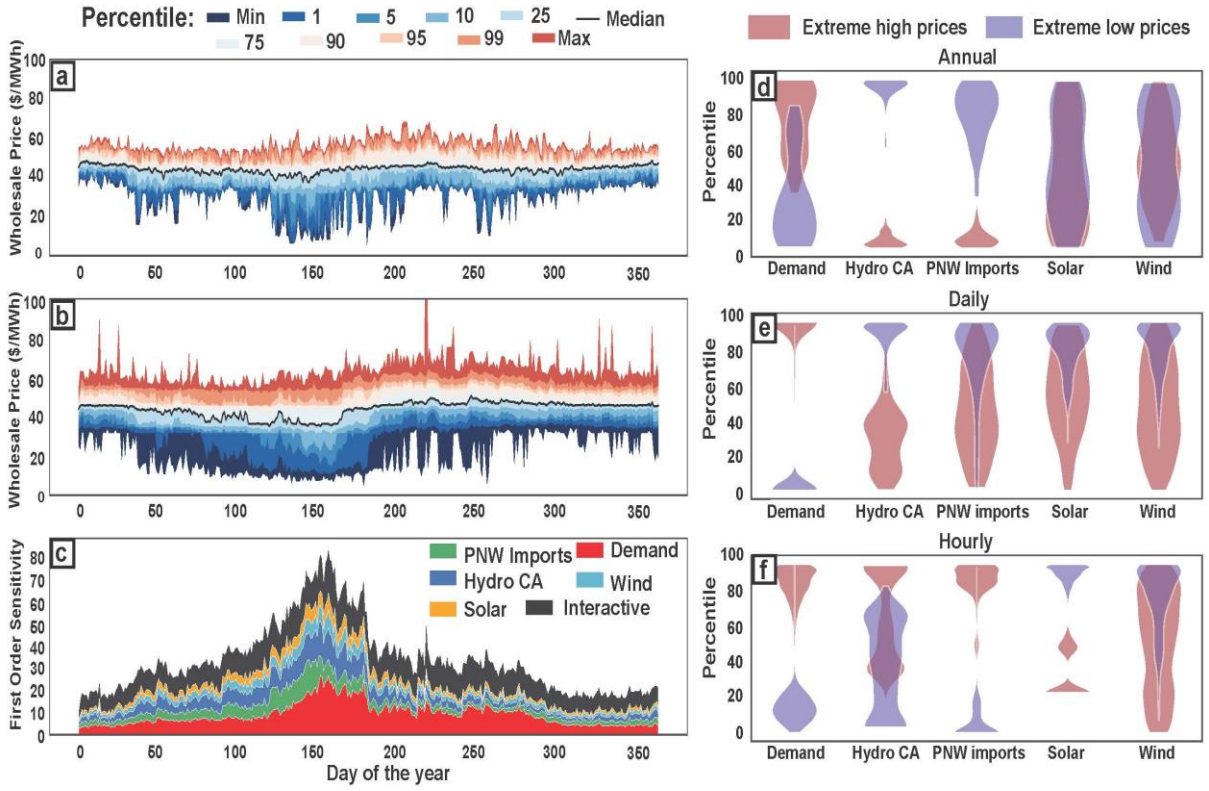

Figure 14: (a) Distributions of daily wholesale prices in CAISO produced using historical hydrometeorological inputs. (b) Distributions of daily wholesale prices in CAISO produced synthetic inputs. (c) First order sensitivity for power system state variables. (d) Power system state variables for yearly extremes. (e) Power system state variables for daily extremes. (f) Power system state variables for hourly extremes.

electricity systems are interdependent, are more likely to experience dry or wet hydrologic conditions simultaneously. Additionally, in California, dry conditions (low hydropower availability) and hot conditions (high electricity demand) are more likely to occur simultaneously. Thus, for the CAISO system, covariance among a few key hydrometeorological state variables across space, acts as a risk multiplier.

In Figures 14 and 15 (and throughout our discussion of sub-annual time scales), we focus

on our evaluation of the CAISO system's performance in terms of wholesale prices and not CO_2 emissions. There are two reasons for not considering CO_2 emissions: 1) prices and emissions show a very strong positive correlation (see Figure 13), so high/low prices can be viewed as an indicator of high/low emissions; and 2) sub-annual dynamics in emissions are likely to pose smaller environmental and/or economic consequences for grid participants relative to volatility in market prices.

Moving from annual to seasonal, daily and hourly time scales, we find important nuances in how different combinations of hydrometeorological states affect system performance. The distribution of daily electricity prices produced using historical (1970-2017) hydrometeorological data (Figure 3a) shows low prices (as low as $5/MWh) are more likely to occur during the spring snowmelt (May-June). In the May-June period hydropower is produced in California and PNW imports are abundant. Historically observed high prices (as high as $68/MWh) are most likely to occur in late summer, when peak snowmelt (hydropower production) has subsided and temperatures (electricity demand) remain very high.

Prices produced using historical data alone (Figure 14a) are a strongly biased underrepresentation of the higher order statistical moments for pricing in CAISO, especially at extreme outer quantiles. Although there is general agreement in terms of mean, seasonality, correlation among state variables, etc., the system's internal variability as captured in the 1000-year synthetic dataset yields a much wider range of extremes in market prices (empirical "min/max" values) (Figure 14b). Underlying these wider extremes are rare but plausible combinations of hydrometeorological conditions that, while reflective of stationary uncertainty (i.e., no climate change), collectively fall outside the recent historical record.

Delta moment-independent sensitivity analysis(Borgonovo, 2007; Plischke, Borgonovo

and Smith, 2013) highlights the dominant factors that influence daily prices (Figure 14c). We find that the first order sensitivity of daily prices to uncertainty in power system state variables (especially electricity demand and West Coast-wide hydropower availability) peaks during spring. This is a notable result, and one that contributes insights beyond previous studies, which have focused mostly on the potential for supply shortfalls to occur in late summer(Miller *et al.*, 2008; Tarroja *et al.*, 2019) (typically a hot, dry period). While we also find greater potential for scarcity (and higher prices) during late summer (Figure 14c), our results strongly suggest that hydrometeorological uncertainty is a more important driver of *market price volatility* during periods of relative abundance (spring). There are two root causes for this phenomenon. First, hydrometeorological uncertainty is greater during spring months (e.g., timing and amount of snowmelt in California and the Pacific Northwest). Second, it is a product of electricity markets' clearing mechanism and the evolving structure of power system supply curves, the bottom of which are increasingly made up of $0/MWh marginal cost wind and solar. During extremely wet years with low spring demand (mild temperatures), hydropower and variable renewables can combine to displace higher marginal cost, fossil-fuel power plants from the market. This causes daily prices to fall sharply.

Time scale is important for understanding how compound hydrometeorological extremes lead to price extremes (Figures 14d-14f). The violin plots across different time scales (annual/daily/hourly) capture extremely high/low prices (defined as $95^{th}/5^{th}$ percentile at an annual time step; $99^{th}/1^{st}$ percentile at daily/hourly time steps) as well as density maps for the five different power system state variables. The progression from annual (Figure 14d) to daily (Figure 14e) and then hourly price extremes (Figure 14f) directly illustrates the relative importance of changes in each state variable.

At the annual scale (Figures 12f and 12d), extreme high prices are driven by low hydropower availability across the West Coast and high electricity demand; low prices experience the opposite. Transitioning to the daily time scale (Figure 14e), very high demand days (e.g., heat waves in late summer) and very low demand days (e.g., 68°F in May) are the most consistent predictors of extreme prices. Extremely low daily prices also consistently map to very high values of California hydropower and PNW imports (often occurring during spring snowmelt), and the availability of wind and solar. Hourly extremes paint a somewhat different picture (Figure 14f). In particular, a significant number of high price hours coincide with very high California hydropower production and hydropower imports from the PNW. This apparent flip in the response of price to hydropower production results because much of the West Coast's hydropower capacity is operated strategically as a "peaking" resource in order to maximize its value. Inexpensive (but finite) hydropower generation is deliberately aligned with hours of high marginal value (prices).

Generation mix dynamics at finer (daily and hourly) resolutions (Figure 15) provide a more detailed mapping for how system operations and market prices are influenced by electricity demand and dynamic resource availability. Note that "imports" shown in Figure 15 are not limited to those from the PNW; they also include some generation imported from the Southwest. The

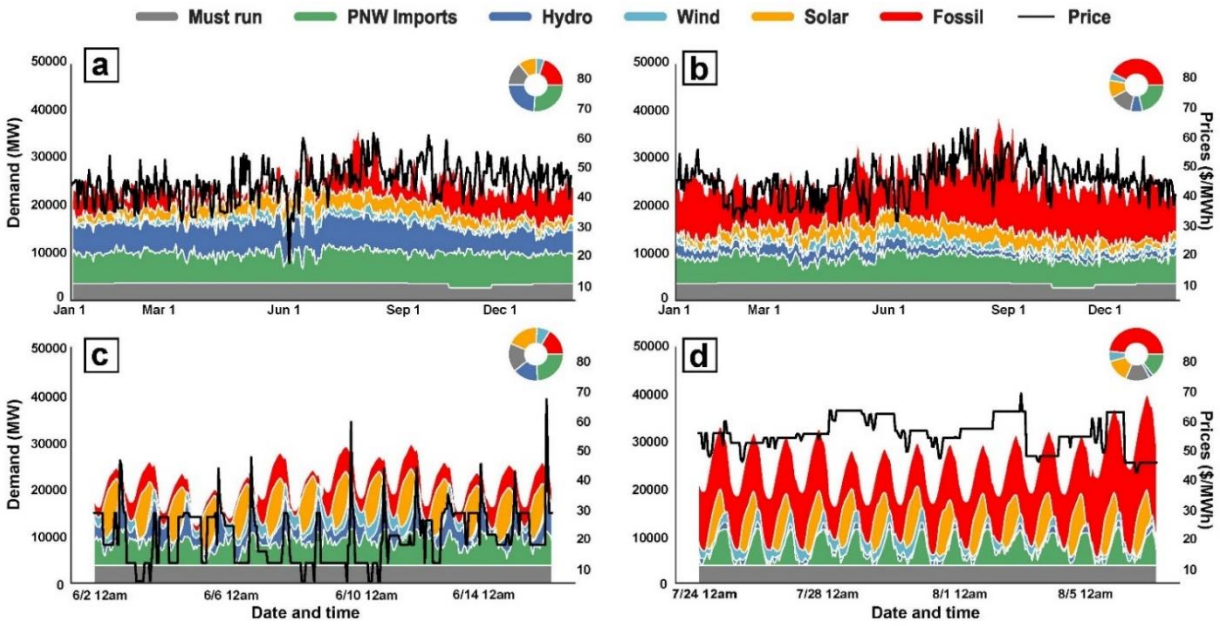

Figure 15: (a) Daily generation mix for the synthetic year with the lowest average price; (b) Daily generation mix for the year with the highest average price; Electricity demand in each day/hour is equal to the (stacked) sum total of all active generation resources. The pie plots in the top right corner of each panel signify the average generation mix used during the period. (c) hourly generation mix for two week period selected from lowest price year; (d) hourly generation mix for two week period selected from highest price year. On both a daily and hourly level, low demand and high hydropower drive prices down; high demand and low hydropower lead to high prices. Renewable generation exerts more control on prices on an hourly scale.

generation mix for the two synthetic years with the lowest (Figure 15a) and highest (Figure 15b) average wholesale price (also discussed in Figures 1-2) show substantial differences. Periods of high demand and low hydropower availability (e.g., August in Figure 15b) increase the need for generation from fossil fuel power plants (mostly natural gas); as this happens, the market price (system "shadow cost") increases. Periods of low demand and plentiful hydropower and variable renewable energy (e.g., beginning of June in Figure 4a) have the opposite effect, with prices falling to $5/MWh when there is a glut of low marginal cost hydropower and renewable energy.

Overall one of the most pronounced differences in the monthly generation mix between the highest and lowest price synthetic years relates to the amount of hydropower and fossil fuel generation used. In the highest price year (Figure 15b), the CAISO market meets 42.4% of its electricity demand using fossil fuel-based power plants, 7% from in-state hydropower and 21.5%

is imported. In the lowest price year (Figure 15a), CAISO only uses fossil fuel-based generation to meet 20% of its electricity demand, 24% comes from in-state hydropower and 26.2% from imports (including a greater amount of imported hydropower from the Pacific Northwest).

Zooming into two critical weeks of the highest and lowest price years, we distinguish how changes in the generation mix shape acute price conditions. In a particularly low price 2-week period (Figure 15c) during the spring of the lowest-price synthetic year, depressed electricity demand (driven by mild temperatures) coincides with high streamflow (an abundance of hydropower), must run generation, and variable renewable energy.

Some fossil-fuel generation remains online, primarily to provide operational reserves, but most is forced out of the market. As a result, the price of electricity frequently falls to $5/MWh, especially during hours when solar irradiance is highest (the "belly" of California's "duck curve"(Denholm *et al.*, 2015)).

Also note that despite lower wholesale prices on average, hourly and daily price patterns during the two-week period in the lowest-price year (Figure 15c) are significantly more volatile than those in a dry, hot period in late summer in the highest-price year (Figure 15d). Natural gas power plants must be turned on and ramped up quickly in the early evening as solar power production declines. In the course of a few hours, prices can jump from near $0/MWh to close to $50/MWh.

3.4 CONCLUSION

There is growing awareness of the economic and environmental hazards that hydrometeorological uncertainty, including compound extreme events, pose for grid operators and electricity market participants. However, previous efforts to characterize these risks probabilistically have fallen short in their consideration of interconnected system topologies and joint uncertainties across correlated variables. For the first time, we isolate the impacts of multiple

hydrometeorological drivers on California's major wholesale electricity market and investigate how compound extremes translate to instances of extreme prices and carbon emissions on the grid. In the course of doing so, we also show that assessing risks associated with compound hydrometeorological events necessitates the use of larger synthetic datasets to access rare, yet plausible system states that have not occurred in the historical record. Controlling for the price of natural gas, we find that time scale strongly effects which combinations of hydrometeorological variables cause extreme prices and emissions. At an annual time scale, simultaneous "hot and dry" or "wet and cool" conditions occurring across the West Coast result in the highest and lowest price/emissions outcomes, respectively. At a daily time scale, we find that very high demand (typically caused by heat waves) drives high price events, while extreme low daily prices are associated with a combinations of low demand (mild temperatures), high hydropower availability, and abundant wind and solar power production. Our modeling confirms a finding in previous studies that West Cost power systems experience the highest prices and greatest threats to reliability during combined hot and dry periods in late summer. However, we find that the market's response to compound hydrometeorological extremes (in terms of altered prices) is most pronounced during spring snowmelt, when demand is typically low (temperatures mild) and there is often an overabundance of power, especially from renewable energy, available on the grid.

It is important to note that the role that different hydrometeorological variables play in power system dynamics today is likely to change in the future as more variable renewable energy is added into the grid. An outstanding challenge remains understanding how future grid configurations, likely comprised of much larger shares of renewable energy, will be vulnerable to compound hydrometeorological extremes. In addition, future work should incorporate growing risks to power systems from discrete events such as coastal and inland flooding and wildfire.

3.5 DATA AVAILIABILITY

The data that were used in this analysis are available at the GitHub repository: https://github.com/romulus97/CAPOW_PY36

REFERENCES

(BPA) Bonneville Power Administration (no date) Historical Streamflow Data.

Belmecheri, S. et al. (2016) 'Multi-century evaluation of Sierra Nevada snowpack', Nature Climate Change. Nature Publishing Group, 6(1), pp. 2–3. doi: 10.1038/nclimate2809.

Borgomeo, E., Farmer, C. L. and Hall, J. W. (2015) 'Numerical rivers: A synthetic streamflow generator for water resources vulnerability assessments', Water Resources Research. doi: 10.1002/2014WR016827.

Borgonovo, E. (2007) 'A new uncertainty importance measure', Reliability Engineering and System Safety, 92(6), pp. 771–784. doi: 10.1016/j.ress.2006.04.015.

CAISO (2018) About Us.

California Energy Commission (2015) 2015 Integrated Energy Policy Report. CEC-100-2015-001-CMF.

California Energy Commission (2019) California Hydroelectric Statistics and Data. Available at: https://ww2.energy.ca.gov/almanac/renewables_data/hydro/index_cms.php (Accessed: 8 May 2019).

CDEC (no date) California Data Exchange Center.

Denholm, P. et al. (2015) Overgeneration from Solar Energy in California. A Field Guide to the Duck Chart. doi: 10.2172/1226167.

Diffenbaugh, N. S., Swain, D. L. and Touma, D. (2015) 'Anthropogenic warming has increased drought risk in California', Proceedings of the National Academy of Sciences, 112(13), pp. 3931–3936. doi: 10.1073/pnas.1422385112.

EPA (2018) Emissions & Generation Resource Integrated Database (eGRID).

Forrest, K. et al. (2018) 'Assessing climate change impacts on California hydropower generation and ancillary services provision', Climatic Change. doi: 10.1007/s10584-018-2329-5.

Franco, G. and Sanstad, A. (2008) 'Climate change and electricity demand in California', Climatic Change, 87(139).

Gleick, P. H. (2016) 'Impacts of California ' s Ongoing Drought: Hydroelectricity Generation', Pacific Institute, (February), pp. 1–14.

Griffin, D. and Anchukaitis, K. J. (2014) 'How unusual is the 2012-2014 California drought?', Geophysical Research Letters, 41(24), pp. 9017–9023. doi: 10.1002/2014GL062433.

Hardin, E. et al. (2017) 'California Drought Increases CO2 Footprint of Energy Production', Sustainable Cities and Society, 28, pp. 450–452.

Harto, C. B. et al. (2011) ‘Analysis of drought impacts on electricity production in the Western and Texas Interconnections of the United States’, Argonne National Laboratory, p. 161. doi: 10.2172/1035461.

Herman, J. D. et al. (2016) ‘Synthetic Drought Scenario Generation to Support Bottom-Up Water Supply Vulnerability Assessments’, 142(11), pp. 1–13. doi: 10.1061/(ASCE)WR.1943-5452.0000701.

Jordehi, A. R. (2018) ‘How to deal with uncertainties in electric power systems? A review’, Renewable and Sustainable Energy Reviews. Elsevier Ltd, 96(June 2017), pp. 145–155. doi: 10.1016/j.rser.2018.07.056.

Kern, J. and Characklis, G. (2017) ‘Evaluating the Financial Vulnerability of a Major Electric Utility in the Southeastern U.S. to Drought under Climate Change and an Evolving Generation Mix’, Environmental Science and Technology, 51, pp. 8815–8823.

Lall, U. and Sharma, A. (1996) ‘A nearest neighbor bootstrap for resampling hydrologictime series’, Water Resources Research, 32(3), pp. 679–693. doi: 10.1029/95WR02966.

Mazdiyasni, O. and AghaKouchak, A. (2015) ‘Substantial increase in concurrent droughts and heatwaves in the United States’, Proceedings of the National Academy of Sciences, 112(37), pp. 11484–11489. doi: 10.1073/pnas.1422945112.

Miller, N. L. et al. (2008) ‘Climate, extreme heat, and electricity demand in California’, Journal of Applied Meteorology and Climatology, 47(6), pp. 1834–1844. doi: 10.1175/2007JAMC1480.1.

Mote, P. W. et al. (2016) ‘Perspectives on the causes of exceptionally low 2015 snowpack in the western United States’, Geophysical Research Letters, pp. 1–9. doi: 10.1002/2016GL069965.Received.

Mureddu, M. and Meyer-Ortmanns, H. (2018) ‘Extreme prices in electricity balancing markets from an approach of statistical physics’, Physica A: Statistical Mechanics and its Applications. Elsevier B.V., 490, pp. 1324–1334. doi: 10.1016/j.physa.2017.09.001.

NOAA (no date) Climate Date Online. Available at: https://www.ncdc.noaa.gov/cdo-web/datasets.

Pathak, P. et al. (2018) ‘Climatic variability of the pacific and atlantic oceans and Western US Snowpack’, International Journal of Climatology, 38(3), pp. 1257–1269. doi: 10.1002/joc.5241.

Plischke, E., Borgonovo, E. and Smith, C. L. (2013) ‘Global sensitivity measures from given data’, European Journal of Operational Research. Elsevier B.V., 226(3), pp. 536–550. doi: 10.1016/j.ejor.2012.11.047.

Ryu, J. H. et al. (2010) ‘Potential extents for ENSO-driven hydrologic drought forecasts in the United States’, Climatic Change, 101(3), pp. 575–597. doi: 10.1007/s10584-009-9705-0.

Sahin, A. D. and Sen, Z. (2001) 'First-order Markov chain approach to wind speed modelling', Journal of Wind Engineering and Industrial Aerodynamics, 89(3–4), pp. 263–269. doi: 10.1016/S0167-6105(00)00081-7.

Scorah, H., Sopinka, A. and van Kooten, G. C. (2012) 'The economics of storage, transmission and drought: Integrating variable wind power into spatially separated electricity grids', Energy Economics. Elsevier B.V., 34(2), pp. 536–541. doi: 10.1016/j.eneco.2011.10.021.

Sengupta, M. et al. (2018) 'The National Solar Radiation Data Base (NSRDB)', Renewable and Sustainable Energy Reviews. Elsevier Ltd, 89(September 2017), pp. 51–60. doi: 10.1016/j.rser.2018.03.003.

Staffell, I. and Pfenninger, S. (2018) 'The increasing impact of weather on electricity supply and demand', Energy. Elsevier Ltd, 145, pp. 65–78. doi: 10.1016/j.energy.2017.12.051.

Stoutenburg, E. D. et al. (2013) 'Variability and uncertainty of wind power in the California electric power system'. doi: 10.1002/we.1640.

Su, Y. et al. (2020) 'An open source model for quantifying risks in bulk electric power systems from spatially and temporally correlated hydrometeorological processes', Environmental Modelling and Software. Elsevier Ltd, 126. doi: 10.1016/j.envsoft.2020.104667.

Tarroja, B. et al. (2019) 'Implications of hydropower variability from climate change for a future, highly-renewable electric grid in California', Applied Energy. Elsevier, 237(May 2018), pp. 353–366. doi: 10.1016/j.apenergy.2018.12.079.

Trabish, H. K. (2017) 'Prognosis megative: How California is dealing with below-zero power market prices', Utility Dive, 11 May. Available at: https://www.utilitydive.com/news/prognosis-negative-how-california-is-dealing-with-below-zero-power-market/442130/.

Turner, S. W. D. et al. (2019) 'Compound climate events transform electrical power shortfall risk in the Pacific Northwest', Nature Communications. Springer US, 10(1). doi: 10.1038/s41467-018-07894-4.

Van Vliet, M. T. H. et al. (2016) 'Impacts of recent drought and warm years on water resources and electricity supply worldwide', Environmental Research Letters, 11(12). doi: 10.1088/1748-9326/11/12/124021.

Voisin, N. et al. (2016) 'Vulnerability of the US western electric grid to hydro-climatological conditions: How bad can it get?', Energy, 115, pp. 1–12. doi: 10.1016/j.energy.2016.08.059.

Voisin, N. et al. (2018) 'Opportunities for joint water-energy management: Sensitivity of the 2010 western U.S. electricity grid operations to climate oscillations', Bulletin of the American Meteorological Society, 99(2), pp. 299–312. doi: 10.1175/BAMS-D-16-0253.1.

Wise, E. K. (2016) 'Five centuries of U.S. West Coast drought: Occurrence, spatial distribution, and associated atmospheric circulation patterns', Geophysical Research Letters, pp. 4539–

4546. doi: 10.1002/2016GL068487.Received.

Woo, C. K. et al. (2017) ‘Electricity price behavior and carbon trading: New evidence from California’, Applied Energy, 204(February), pp. 531–543. doi: 10.1016/j.apenergy.2017.07.070.

Zhou, T., Voisin, N. and Fu, T. (2018) ‘Non-stationary hydropower generation projections constrained by environmental and electricity grid operations over the western United States’, Environmental Research Letters, 13(7). doi: 10.1088/1748-9326/aad19f.

Zohrabian, A. and Sanders, K. (2018) ‘Assessing the impact of drought on the emissions- and water-intensity of California’s transitioning power sector’, Energy Policy, 123, pp. 414–420.

Zscheischler, J. et al. (2018) ‘Future climate risk from compound events’, Nature Climate Change. Springer US, 8(6), pp. 469–477. doi: 10.1038/s41558-018-0156-3.

Zscheischler, J. and Seneviratne, S. I. (2017) ‘Dependence of drivers affects risks associated with compound events’, Science Advances, 3(6), pp. 1–11. doi: 10.1126/sciadv.1700263.

CHAPTER 4: THE EFFECTS OF RETAIL LOAD DEFECTION ON A MAJOR ELECTRIC UTILITY'S EXPOSURE TO WEATHER RISK

4.1 INTRODUCTION

In the electric power sector, hydrometeorological uncertainty and extremes can negatively impact the functionality of generation resources and cause large changes in customer demand(Pappas *et al.*, 2008; J Kern and Characklis, 2017). Streamflow, which acts as a 'fuel' for hydropower production and a critical coolant for thermal power plants, is subject to hydrologic variability. Electricity demand, which is strongly affected by heating and cooling needs, is directly influenced by deviations in air temperatures above and below the human comfort range (18.3 degrees C or 65 degrees F), with heat waves and cold snaps typically causing spikes in demand. By affecting both supply and demand for electricity, variation in hydrometeorological conditions can also be a source of financial stress for power system participants(Deng, 1999; Deng and Oren, 2006). For example, hydrologic conditions directly influence revenues for hydropower-owning utilities and, in combination with air temperatures, can significantly influence prices in wholesale electricity markets. Utilities have traditionally made use of a wide range of tools to manage exposure to these risks, ranging from heating/cooling degree-day hedging contracts that protect against air temperature deviations from expected levels to "parametric" insurance that protects against hydrologic variability(Foster, Kern and Characklis, 2015; Kern, Characklis and Foster, 2015).

Similar to other businesses, electric utilities are also exposed to market and regulatory risks(Taminiau *et al.*, 2019; Deng *et al.*, 2020). For example, in recent years, the combination of

policy pressure, market deregulation and falling renewable energy costs have led to a steady transition away from fossil fuel based generation in many U.S. power markets(Denholm *et al.*, 2015a; Su, Kern and Characklis, 2017). This has created many new risks for some incumbent utilities, including reduced market share. Ostensibly, risks for utilities from weather and the energy transition may seem independent, requiring separate management strategies, however, it is possible (perhaps likely) that these risks interact in complex ways, with underlying changes in one area leading to altered exposure in the other. For example, increased reliance on wind and solar power could increase a utility's exposure to uncertainties in wind speeds and solar irradiance(Collins *et al.*, 2018). Financial distress caused by harmful weather and climate events (e.g. wildfire in California) can also result in lower credit ratings and an increased cost of borrowing, potentially leading to higher costs for new renewable energy projects(BlackRock, 2019; McKinsey Global Institute, 2020).

A less well-understood example is the interplay between a utility's exposure to weather risk and "load defection", i.e., the gradual diminution of a utility's retail load base (demand) due to customer use of energy efficiency measures or increased use of self- or third-party owned solar panels. Utility competition with community choice aggregations (CCAs), local government entities that procure electricity on behalf of retail customers within a certain geographical area can also have an impact. While participation in CCAs is voluntary, in eight U.S. states (CA, IL, MA, NJ, NY, OH, RI and VA) they directly compete with incumbent utilities for customers. By sidestepping a traditional utility's generation portfolio, CCAs and their customers can (in theory) purchase their electricity from less polluting sources, including wind and solar farms.

The potential negative effects of load defection on incumbent utilities' financial standing have been noted previously(Gunther and Bernell, 2019; O'Shaughnessy *et al.*, 2019). However,

no consideration has yet been given to the effects defections can have on an electric utility's exposure to weather risk – and vice versa. Utilities participating in competitive markets for electricity generally have three main revenue sources: 1) a generation business that sells electricity produced from the utility's own power plants into a wholesale market); 2) a transmission business that charges grid participants for the use of utility-owned high voltage transmission lines; and 3) a retail distribution business that purchases electricity from the wholesale market and sells this to end users(Bryant, Straker and Wrigley, 2018). If utilities' retail electricity businesses contract due to load defection, the relative importance of other revenues sources (i.e. transmission and/or wholesale generation) may increase. For some utilities, this could alter exposure to weather risk by strengthening or weakening the correlation between hydrometeorological conditions and financial outcomes, and/or by increasing weather-caused financial variability as a proportion of a utility's (shrinking) overall business.

Given the rapid rates at which load defection is now occurring at some utilities, significant changes in utilities' financial exposure to weather risk may occur quite quickly (in a matter of a few years(JOHN, 2017; Kennedy and Rosen, 2020)). At least in terms of rate-of-change, this is somewhat in contrast to the projected impacts of climate change, which are expected to increase utilities' physical and financial exposure to weather phenomena over decades(Franco and Sanstad, 2007; Sautter and Twaite, 2009; Nierop, 2014; Omid Mazdiyasni and AghaKouchak, 2015; Bartos *et al.*, 2016; Dominique Bain and Acker, 2018; Kraft, 2018). Here, we perform a series of computational modeling experiments to better understand the effects of load defection on a major utility's financial exposure to weather risk. The broader value of this work is in showing how changing revenue structures and business models can impact a utility's exposure to hydrometeorological uncertainty and extremes. Our results highlight new complexities involved

in helping utilities to find the most effective ways to hedge risk to maintain their financial stability.

4.2 METHODS

4.2.1 Test Bed

We focus our analysis on Pacific Gas and Electric (PG&E), the largest power and transmission utility in California. PG&E participates in the deregulated wholesale market administered by the California Independent System Operator (CAISO), technically as three separate entities, all owned by the same holding company: 1) a generation business that sells electricity produced from PG&E-owned power plants, and electricity procured from other sources, into a competitive wholesale electricity market. Generation sold in this manner is valued at a floating price determined by the interaction between supply and demand in the wholesale market; 2) a transmission business that delivers electricity to end users; and 3) a retail business, which purchases electricity from the wholesale market (also at the wholesale price) and sells it to its own retail customers(Pacific Gas and Electric Company, 2019). Since 2014, PG&E has been experiencing retail load defection from customer uptake of rooftop solar and competition from CCAs(Gunther and Bernell, 2019; O'Shaughnessy *et al.*, 2019; Kennedy and Rosen, 2020), and it is projected that PG&E could lose over 80% of its retail load within three to five years(JOHN, 2017). If PG&E does lose a majority of its retail load, risks in PG&E's wholesale generation and transmission businesses may begin to exert greater influence on the utility's revenues and measures of its financial stability (e.g. credit rating), which have direct bearing on critical factors such as borrowing power and interest rates.

Weather risk is already a key concern in both PG&E's transmission and wholesale generation businesses. Air temperatures strongly influence demand for electricity in PG&E's footprint, thus also driving demand for transmission services. In PG&E's wholesale generation business, its largest source of self-owned capacity is a fleet of hydroelectric dams located in California's Sierra Nevada Mountains. These dams provide operationally flexible (i.e. they can be ramped up/down

with little penalty), low carbon generation, however, they are also highly dependent on hydrologic conditions, with high/low snowpack years leading to more/less hydropower production. As PG&E's retail business shrinks, the relative importance of its transmission and wholesale generation businesses will grow. There is particular interest in understanding how the utility's overall exposure to hydrometeorological conditions (including hydrologic extremes) could change– not due to changes in air temperatures and streamflow dynamics, per se (although this is likely to occur as well due to climate change) – but rather, an evolving marketplace.

4.2.2 Modelling Framework and Experimental Design

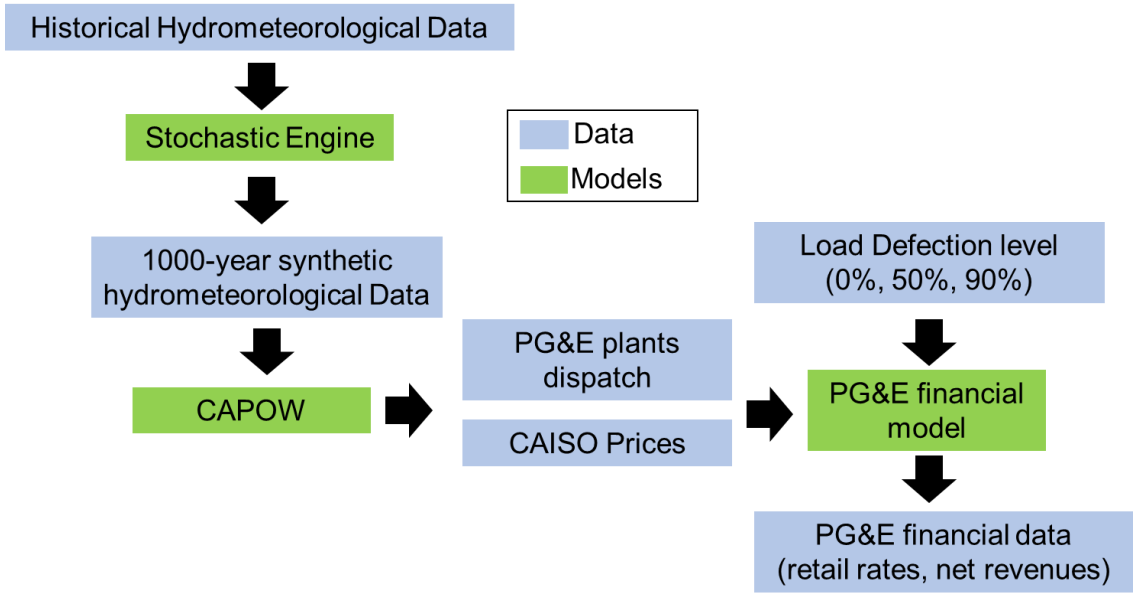

Figure 16: Modelling framework including data inputs/outputs and model modules

We use a system-based modelling approach to simulate CAISO market operations and the financial operations of PG&E's electricity businesses (wholesale generation, transmission and retail distribution) (Figure 16). To simulate the CAISO wholesale electricity market, we use the California and West Coast Power system (CAPOW) model, which is an open source stochastic simulation framework designed specifically for evaluating the effects of hydrometeorological

variables on the U.S. West Coast bulk power system. CAPOW is Python-based and all source code and data are freely available online; validation and application of the model in other studies can be found in Su et al. (2020a)(Su *et al.*, 2019), Kern et al. (2020)(Kern, Su and Hill, 2020) and Su et al., (2020b)(Su, Jordan D Kern, *et al.*, 2020). We couple the CAPOW model with a representation of PG&E's business operations to simulate utility financial performance under hydrometeorological uncertainty. We run CAPOW and then the PG&E business model in a sequential fashion, first capturing the effects of weather and streamflow conditions on system-wide supply, demand, and wholesale prices in the CAISO market. CAPOW also simulates the hourly dispatch of all generating units participating in CAISO, including those owned and contracted by PG&E. We then model PG&E's costs and revenues across the three core components of its business. In this work, we focus on PG&E's "net revenue" as the primary financial performance metric. Net revenue is defined as the difference between annual revenues and costs (costs include debt service and a 10% return on equity for shareholders).

The aim of this work is to investigate how PG&E's financial exposure to hydrometeorological variables will change as their customer base declines, but their generating capacity remains constant as a result of long-term investments in generation assets. To achieve this, we simulate PG&E's operations under three different retail load scenarios: 2018 levels (assumed to be 0% load defection), 50% load defection, and 90% load defection. We choose 2018 load levels as a starting point instead of 2019 due to increased sectoral data availability. In our modeling, we assume load defection comes only from competition with CCAs, as opposed to customer owned/sited distributed energy resources (e.g., solar). This assumption aligns with observed historical data (see Figure A2 in the Appendix). We evaluate PG&E's net revenues on an annual basis, tracking the correlation between weather variables and financial performance to

determine if these statistical relationships change under possible future levels of load defection. We focus on PG&E's exposure to uncertainty and extremes in air temperatures and streamflow, as previous research suggests that wind speeds and solar irradiance do not (yet) influence market prices on an annual scale at current installed wind and solar power levels(Su, Jordan D Kern, *et al.*, 2020).

4.2.3 California and West Coast Power (CAPOW) model

The geographical scope of the CAPOW model covers two wholesale power markets including CAISO, which covers most of the California, and the Mid-Columbia (Mid-C) power market, which covers much of the U.S. Pacific Northwest. CAPOW has 2 core components:1) a stochastic engine; and 2) a zonal unit commitment economic dispatch (UC/ED) model(Su *et al.*, 2019).

The stochastic engine takes historical hydrometeorological timeseries from multiple sites and uses these data and a range of statistical and stochastic modeling approaches to generate an

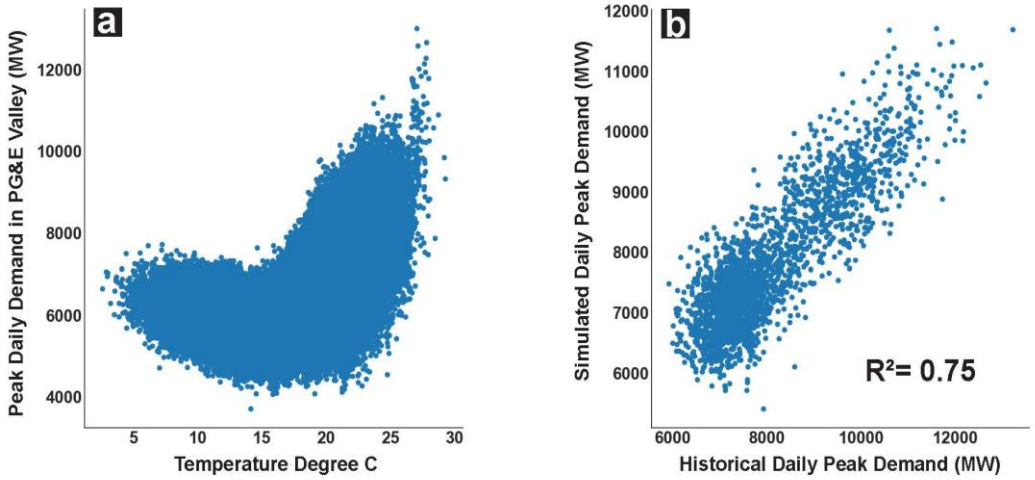

Figure 17: (a) An example of temperature effects on system demand. Higher temperature corresponds to higher electricity demand due to cooling needs whereas low temperature increases electricity demand by increase heating needs. (b) Validation of the simulated PG&E valley (PG&E footprint outside of San Francisco Bay Area) demand using temperature against historical observations.

expanded 1000-year synthetic time series. Historical data come from 17 major regional airports in

the NOAA Global Historical Climatological Network (air temperature and wind speed data), 7 different National Solar Resource Database sites (irradiance) and 105 streamflow gauges throughout the West Coast. The stochastic engine, which has been thoroughly validated in our previous research(Su, Jordan D. Kern, *et al.*, 2020), is able to produce synthetic time series that capture the statistical properties (moments, spatial and temporal autocorrelation) across all variables (More details in the Appendix). The advantage of using synthetic time series is that the expanded dataset can capture uncertainties and extremes outside the limited historical record.

Synthetic air temperature and wind speed data are then used to simulate daily peak and hourly electricity demand in the CAISO market, including the PG&E footprint, using multivariate regressions (Figure 17). Errors are represented by vector autoregressive models that capture spatial and temporal correlations across demand sites. Similar methods are used to simulate wind and solar power generation on a zonal level at an hourly time step. Hydropower production is modelled using a hydrologic mass balance model for the dam-reservoirs in the Federal Columbia River Power System (Pacific Northwest), Willamette River basin (Oregon), and Sacramento, San Joaquin and Tulare Lake basins (California). A large portion of the California dams do not, however, have publicly available rule curves; thus we use a differential evolutionary algorithm to search for the best fitting rule curve for those dams(Su *et al.*, 2019).

Given the time series inputs described above, CAPOW then simulates the hourly dispatch of every power plant in the system by minimizing the system wide production cost associated with meeting hourly demand for electricity and operating reserves, subject to generator-specific and system-wide operating constraints. The UC/ED model is structured as an iterative Mixed Integer Programming (MIP) with an operating (“look-out”) horizon of 48 hours. Simulating the UC/ED component of the model generates hourly zonal electricity prices in terms of $/MW, plant level

carbon emissions (tons of CO_2) and hourly plant level generation amounts (MW).

4.2.4 PG&E business model

The PG&E business model simulates the utility's financial operations using publicly available data from its annual financial reports(Pacific Gas and Electric Company, 2017, 2019). PG&E's electricity business is comprised of three quasi-independent entities: 1) a wholesale generation business; 2) a transmission business; and 3) a retail distribution business. We model dynamic costs and revenues for each. PG&E's wholesale generation business can be subdivided into: 1) self-owned generation (i.e. electricity produced by power plants that PG&E owns); and 2) third party contracts (e.g. long-term procurement of generation from assets owned by other entities, most in the form of power purchase agreements (PPAs) for renewable energy). PG&E owns several hydroelectric dams totaling 2860 MW, two natural gas power plants (1100 MW) and 1 nuclear plant (2240 MW) (Table 4). In this study, we assume PG&E's 2019 third party contracts, at least in terms of the volume and types of resources involved. Notably, PG&E's renewable energy PPAs tend to be much more expensive than the average simulated market price in CAISO (about $45/MW), with many contracts priced at roughly $140/MW(Dudziak, Ewing and Horn, 2019). For PG&E's remaining third party contracts, the exact terms and price structure for those contracts are not public, so we initially assume flat rates of $45/MW for electricity procured in this way, which is the average wholesale price over our 1000 synthetic runs with natural gas prices fixed at $4.5/MMBtu.

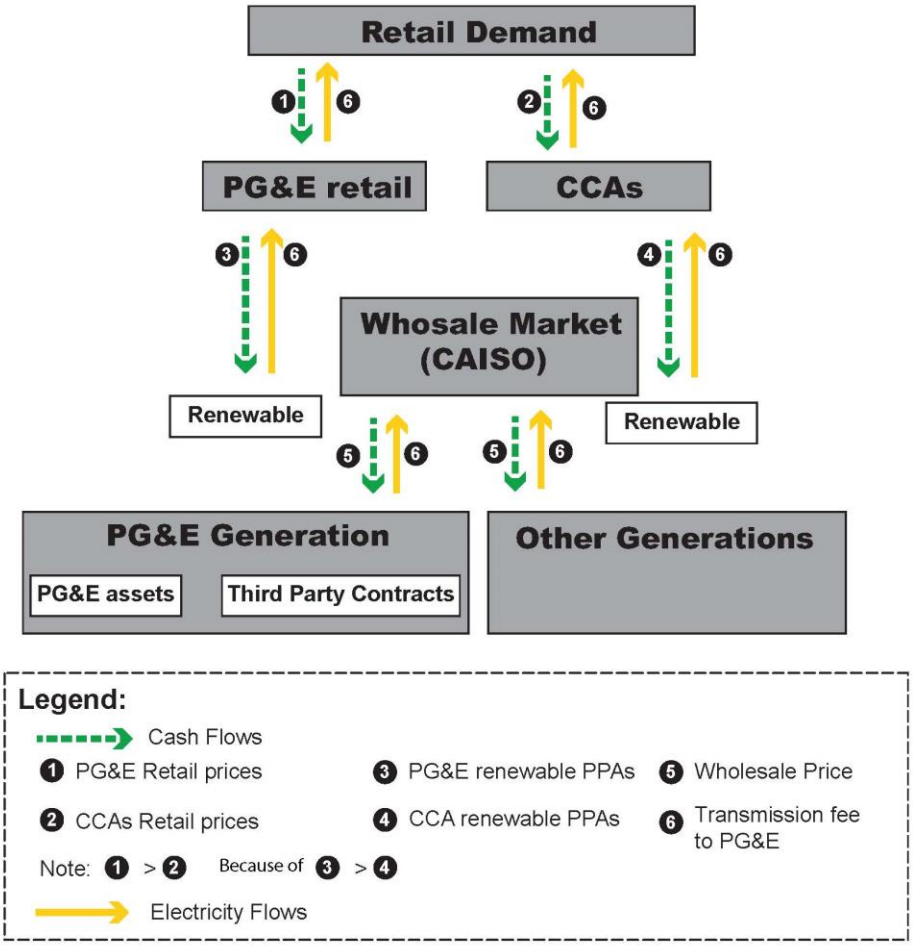

Figure 18: Power and cash flow in the wholesale and retail system. The relationship of 3 parts of the PG&E business, namely wholesale generation, retail and transmission are shown. The CCAs outcompetes PG&E retail business due to cheaper renewable contracts signed in recent years.

Even if a majority (or all) of the generation produced by PG&E's generation assets (both self-owned and third party contracts) is ultimately purchased by its retail distribution business, PG&E technically must first sell generation from its power plants into the wholesale market, where it competes with other generators all of whom set their bids into the market on the basis of cost then purchase the power back from wholesale market to meet its own customers retail demand. The detailed cash and electricity flow can be seen on Figure 18. To model PG&E's generation business, we identify the generation assets owned by PG&E and thermal generation plants associated with third party contracts in the CAPOW model. We model production from PG&E's

wind, solar and hydropower PPAs proportional to overall production of these resources in the larger CAISO system. Based on CAISO prices and modeled dispatch results, we calculate costs (e.g. fuel) and revenues associated with PG&E selling electricity into the wholesale market.

Table 4. PG&E's generation assets and third party contracts for 2019.

Self-Owned Generation Mix		
Type	**Capacity (MW)**	**Number of Units**
Nuclear	2240	2
Hydroelectric dams	2680	103
Pump Storage	1212	3
Fossil Fuel-fired	1100	12
Photovoltaic	152	13
Third Party Contracts (GWh)		
		2019
Renewable		9276
Non-Renewable		4530
Large Hydroelectric		1797

PG&E's transmission revenues come from distribution of electricity to its own retail customers as well as CCA customers living within PG&E's geographical footprint. Each customer that receives electricity from a PG&E owned line is charged a flat rate of $0.126/kWh for the use of PG&E's transmission infrastructure (Table 4). PG&E's revenues from its transmission business accrue at this rate based on its delivery of electricity to customers in its territory. PG&E's own customers pay for both electricity and transmission service, proportional to their own demand;

CCA customers only pay for transmission service, also proportional to their own demand.

PG&E's retail distribution business earns revenue from the sale of electricity to customers across its four major customer classes (commercial, industrial, residential, agricultural). Demand from each sector is disaggregated from total PG&E demand based on historical monthly demand fractions. PG&E's retail rate structure is complex, with roughly 100 different rate structures across different customer groups and use cases. In our model, we assume the most common seasonal rate structures for each customer class (Table 5). PG&E defines summer as the months of May, June, July, August, September, and October; they define winter as January, February, March, April, November and December. The summer rate is generally higher than the winter rate across the four sectors. The only exception is the industrial sector rate, which is the same throughout the year.

We also model the five main cost components of PG&E: 1) fuel costs from its generation assets; 2) payments to third party generation contracts; 3) purchases from the wholesale market; 4) operation and maintenance costs (O&M); and 5) debt service and 10% return on equity for shareholders, assuming a depreciated asset base of $30 billion(Pacific Gas and Electric Company, 2019). Fuel costs are calculated based on generator unit heat rates and dispatched generation simulated from CAPOW. Payments to third party contracts are assumed to accrue at a flat rate ($140/MW for renewables and $45/MW for other sources). Purchases from the wholesale market are calculated as PG&E's calculated retail demand in every hour multiplied by the floating market price in the CAISO market. Lastly, O&M, debt service payments and return on equity for shareholders are fixed equal to values reported by PG&E for 2019(Pacific Gas and Electric Company, 2019). From 2016-2019, these reported values from PG&E changed little year-to-year. In our modeling, we assume that these values would also remain static under future load defection levels.

Table 5. Rate structure used to model the business operation of PG&E.

	Electricity Rate ($/kwh)	
	Summer (May-Oct)	Winter (Jan-Apr, Nov, Dec)
Residential	0.27029	0.21024
Commercial	0.25069	0.19024
Agriculture	0.3076	0.23722
Industry	0.1055	0.1055
	Transmission Rate ($/kwh)	
Transmission rate	0.127	

4.3 RESULTS AND DISCUSSION

4.3.1 Changes in costs and revenues

Figure 19 breaks down PG&E's average cost and revenue components under three different customer load levels: 2018 load levels, following 50% load defection, and following 90% load defection. The "outer" circles of pie charts shown in Figure 19 represent PG&E's revenue sources; "inner" circles represent cost components. Figures 19d and 19e, which correspond to load defection of 50% and 90%, respectively, show how the contributing fraction of each revenue and cost component changes, relative to current load levels. Note that these pie charts assume that PG&E's retail rates stay the same (i.e. they are not increased by the utility to compensate for lower retail demand).

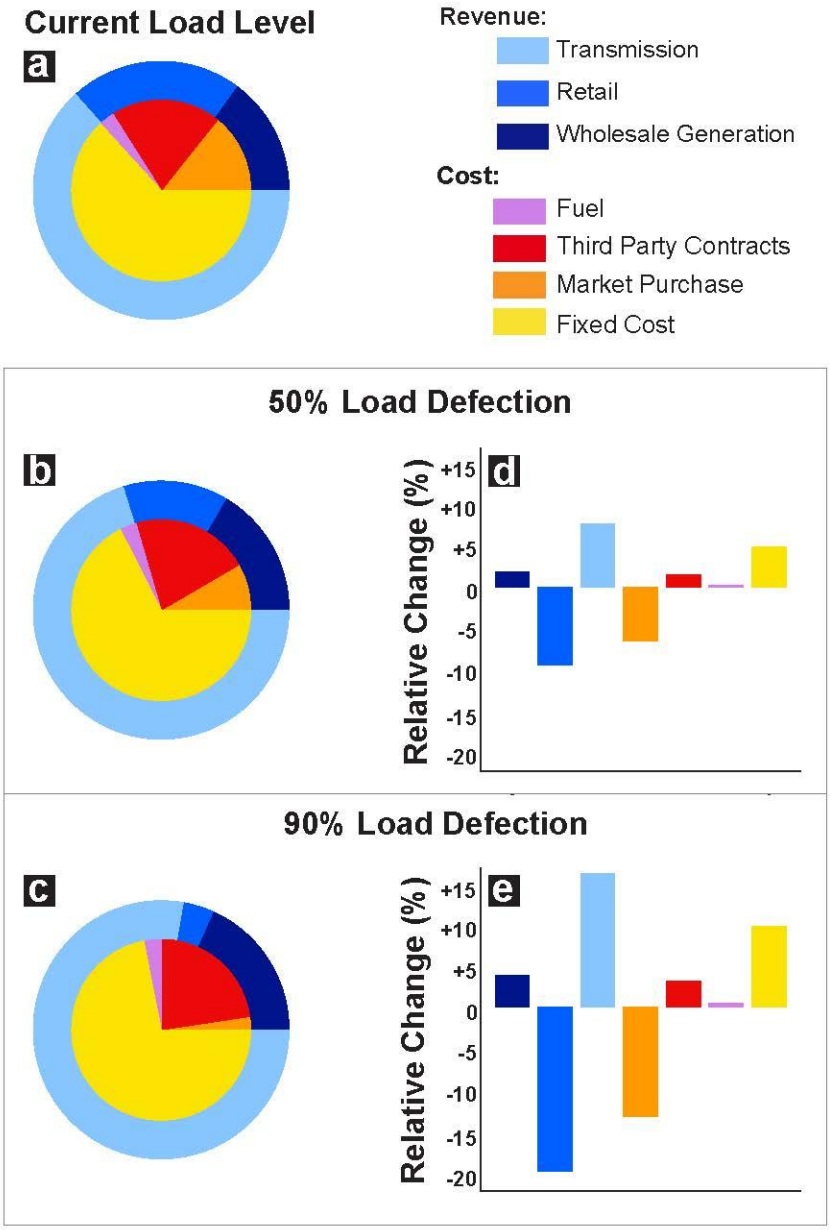

Figure 19: PG&E revenue and cost breakdown for current load levels, 50% load defection and 90% load defection scenarios.

Our modeling results confirm that load defection could cause significant changes in the make-up of PG&E's cost and revenue components. Retail revenues are currently PG&E's second largest source of revenue after transmission revenue. Unsurprisingly, when 90% of PG&E's customers leave the system, the utility's retail business becomes its smallest source of revenue. At the same time, load defection increases the relative importance of its wholesale generation and

transmission businesses, even as revenues from wholesale generation and transmission stay roughly the same in an absolute sense (see Figure 20)Wholesale revenue is selling self-generated electricity to the market is independent from load defection, because the underlying generating assets in PG&E remain the same. Thus the ability to sell electricity to wholesale market is unaffected. Transmission revenue on the other hand, depends the electricity demand in the entire region, which also is not affected by load defection. Overall regional demand can be reduced if the distributed generation resources becomes more popular.

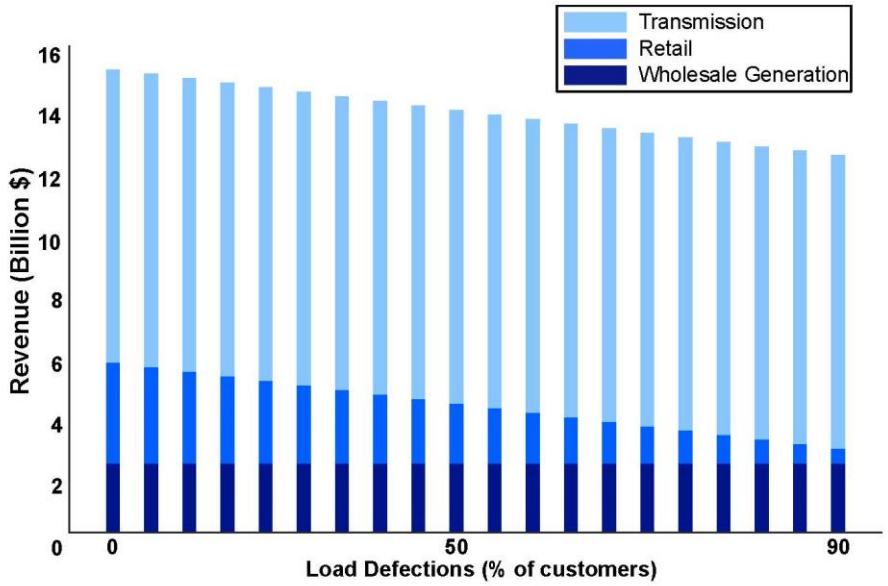

Figure 20: Overall revenue decline as load defection increases

Figure 20 also shows impacts to PG&E's cost components. Purchases from the wholesale market decrease in both a relative and absolute sense. As PG&E's retail load decreases, the utility transitions from being (on average) a net buyer of electricity in the wholesale market to a net seller. In other words, as PG&E's retail load decreases, the utility more frequently experiences a "surplus" of wholesale generation from its self-owned and contracted resources. We also see that, third party contracts and fixed costs (O&M, debt service, etc.) increase as a percentage of total costs, despite not increasing in an absolute sense.

One of the most important effects of load defection is the reduction in overall revenue for

PG&E (Figure 20). The reduction in retail revenue experienced by PG&E outweighs a slight increase in revenues from wholesale generation, leading to an overall decline in revenue from around $16 billion at current load levels to $13 billion with 90% load defection. In theory, PG&E aims to be net revenue natural ($0 net revenue) after accounting for all the costs and shareholder's return on equity (ROE). Losses of this magnitude would put considerable financial pressure on the utility to raise rates on customers so that they could maintain a reasonable return on equity for shareholders, a topic explored in the next section.

4.3.2 Increasing rates and increasing uncertainty

Traditionally, regulated electric utilities (acting with approval from utility commissions) have been able increase electricity rates on customers to counter revenue deficits(California Public Utilites Commission, 2020). It is not clear, however, that this will be a viable strategy in the future if/when more and more customers defect from PG&E. In Figure 21, we demonstrate the potential effects from retail customer losses on PG&E's average retail rates. At each level of load defection and for each simulation year considered, we calculate the $/kWh retail electricity rate required to cover PG&E's annual operating costs (including debt service and a 10% return on equity). No changes are assumed for PG&E's transmission rate, because PG&E's revenues from its transmission service remain unchanged as long as customers continue have power on PG&E lines, even if that electricity is sold by a CCA.

The blue boxplots in Figure 21 represent the distribution of electricity rates required to reach net revenue neutral at each load level across 1000 single-year model realizations. As load defection increases, PG&E's electricity rates need to increase dramatically to counter the associated decline in retail revenues. Our results indicate that at 90% load defection levels, customers remaining in PG&E's pool would need to pay electricity rates of over $210 /MWh (i.e.

$0.21/kWh), which is 328% of current electricity rate ($64 /MWh or 0.064 /kWh), on average to compensate for PG&E's reduced retail revenue. Adding associated transmission costs ($0.127/kWh) would bring the overall retail rate for PG&E customers to around $0.337/kWh. Such substantial increases in electricity rate will driver more people to choice cheaper options such as joining CCAs and/or adopting distributed energy system by installing solar panel on their roofs. The further depleted customer base would raise the prices even higher which continues the positive feedback loop. Such phenomenon is part of the widely discussed "death spiral"(Castaneda *et al.*, 2017; Laws *et al.*, 2017).

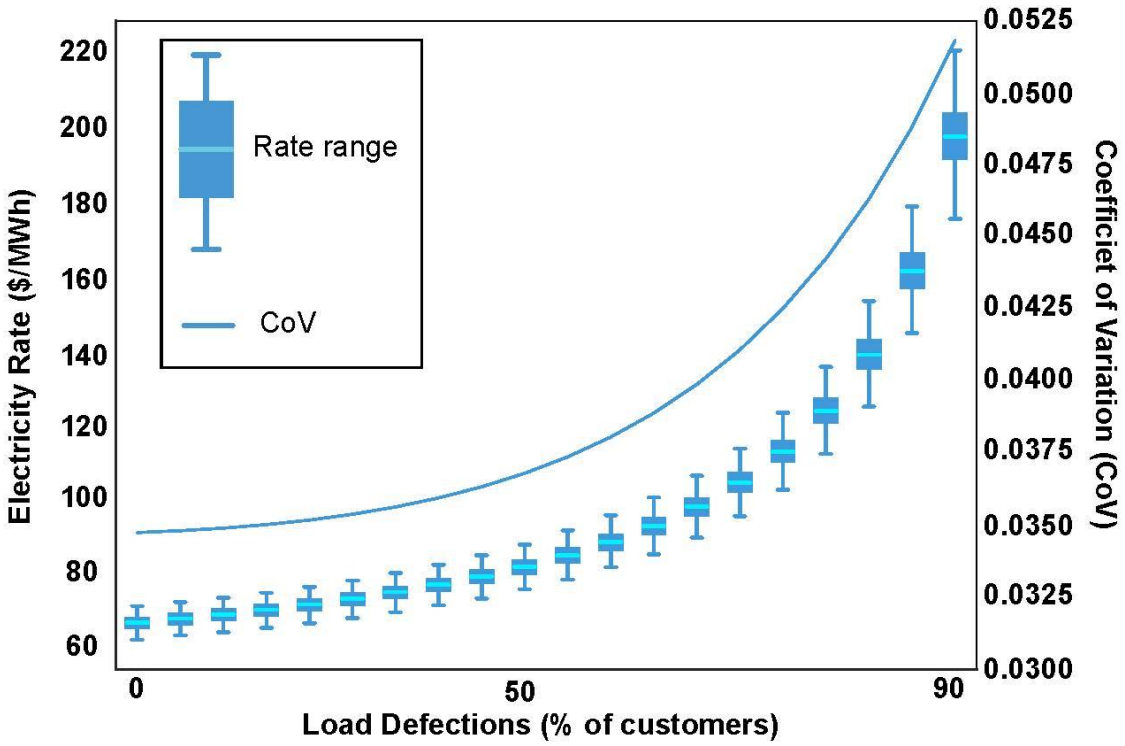

Figure 21: Simulated rate change as customer base decreases. The rate needs to increase in an exponential way to counter act the decreased retail demand. The rate variation and coefficient of variance will also increase dramatically.

Another important pattern we see is that year-to-year variation in the rate required (i.e. the range of the "whiskers") increases significantly as a function of load defection. This increase in uncertainty is also quantified using a coefficient of variation measure on the secondary y-axis. At

any given load level, variability in the rate required is purely a function of uncertainty in weather (especially air temperatures and streamflows), which directly influences CAISO market prices and PG&E's costs and revenues. It is important to note that the increase in financial uncertainty shown in Figure 21 is not caused by an increase in the year-to-year fluctuations in PG&E's costs and revenues. Rather, due to PG&E's shrinking retail business, as shown in equation 1, even as net revenue variation maintains the similar level, the electricity rate variation will increase. . Consequently, each remaining customer in PG&E's system needs to shoulder a greater share of this variability. In theory, this could lead to greater year-to-year swings in electricity prices for remaining customers. In reality, PG&E may be somewhat limited in its ability to immediately raise/lower retail rates to address unexpected revenue surpluses/shortfalls caused by its exposure to weather risk. Thus, it could be reasonably assumed that a significant share of share of this financial uncertainty would fall on shareholders, as opposed to customers alone. This makes understating the changing nature of PG&E's financial exposure, especially as it relates to weather risk, much more important.

$$Electriciy\ rate\ variation = \frac{Net\ revenue\ varaition}{Retail\ load} \quad (1)$$

4.3.3 Net revenue and weather variables

In the following sections, we explore how load defection could fundamentally alter PG&E's financial exposure to hydrometeorological uncertainty, including extremes. Previous studies(Mureddu and Meyer-Ortmanns, 2018; Su, Jordan D Kern, *et al.*, 2020) have shown that air temperatures (which drive interannual variability in demand) and hydrologic conditions (which control the availability of hydropower) are the most dominant environmental factors that influence operations and market prices in the CAISO system. Previous studies have also shown that PG&E(Kern, Su and Hill, 2020) is strongly influenced by both air temperatures and streamflows.

Thus, our analysis focuses on PG&E's changing financial exposure to these two weather variables.

In the remaining analysis, we assume that PG&E is able to recover retail revenue losses

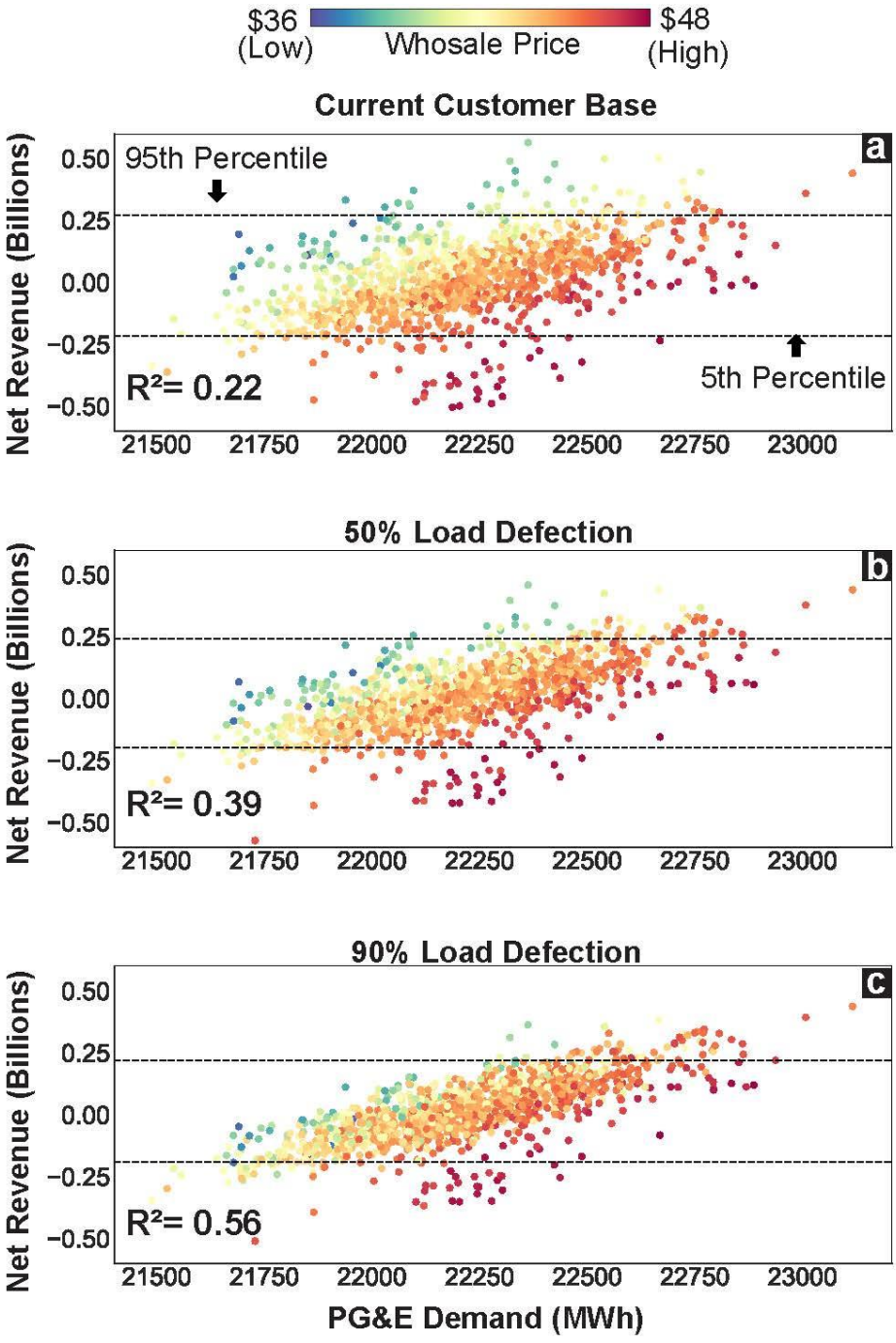

Figure 22: PG&E system demand's effect on PG&E net revenue. The correlation between system demand and net revenue increases as customers leave the system.

caused by load defection. As PG&E's retail load declines, we add a fixed fee for all retail and transmission customers to ensure that at any load level, the utility's net revenue (after making debt service payments and issuing a 10% return on equity to shareholders) is $0 on average, across 1000 single year simulations. By 'guaranteeing' PG&E's cost recovery in an average year, we can then isolate the effects of hydrometeorological uncertainty on their financial performance at different load levels without introducing any confounding variables.

Figure 22 shows the relationship between total system demand in the PG&E footprint (x-axis) and modeled annual net revenues for PG&E (y-axis) under the three different load levels considered (current, 50% defection, 90% defection). Note that demand here includes electricity consumed by CCA customers who are within the PG&E footprint, even though PG&E does not sell to those customers. At current load levels (Figure 7a), net revenues are positively correlated with system demand, i.e. higher demand corresponds to higher net revenues and lower demand corresponds to lower net revenues. Note that when we control for a given level of electricity demand (take a vertical transect of Figure 22a), lower market prices are generally better for net revenue. This actually reflects PG&E's exposure to hydrology (wet years simultaneously decrease market prices and increase hydropower production at PG&E's dams) and wholesale prices. At a given demand level, lower wholesale price means that it is cheaper to purchase electricity from the market to meet the retail demand. At the same time, this reflects more hydropower revenue generated from PG&E's hydroelectric facilities (see Appendix for additional exploration of relationship between hydrologic conditions, hydropower production, and market prices in CAISO). The additional sales from hydro in wet years more than compensate for the reduction in wholesale revenue that resulted from the lower prices. More detailed discussion on hydrologic

exposure is presented later in this section.

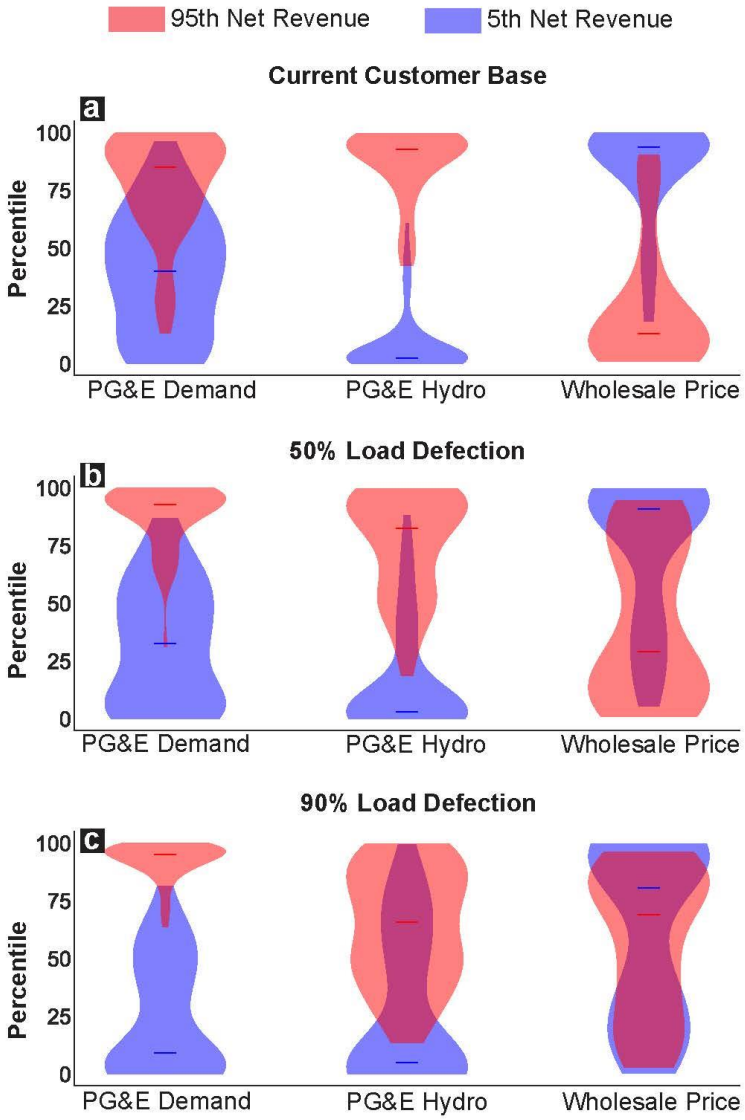

Figure 23: Density plots of electricity demand, hydropower production and wholesale electricity prices of extreme net revenue simulations (5th and 95th percentile) under current, 50% and 90% load defection levels.

However, as PG&E's retail customer base declines (going from Figure 22a to Figure 22c), vertical stratification due to market prices (hydrology) collapses and the correlation between CAISO system demand and PG&E's net revenues becomes stronger (R^2 changes from 0.22 to 0.56). This indicates that air temperatures (which drives electricity demand in the PG&E footprint) will become a better indicator of net revenue. Recall Figures 19 and 20 where load defection

would lead to transmission revenue accounting for an even higher percentage of overall revenue (over 75% on average); this directly contributes to the increased correlation between demand within PG&E's footprint and its net revenue.

Figure 23 shows density plots of electricity demand, hydropower production, and wholesale electricity prices under the three different load defection levels. These plots only show simulation years with extremely high (95^{th} percentile) PG&E net revenues and extremely low (5^{th} percentile) net revenues, colored in red and blue respectively. Looking only at the distributions of electricity demand in the PG&E footprint, we see that with increasing load defection (going from Figure 8a to Figure 8c) years of extremely high/low net revenues gradually concentrate around years of extremely high/low demand. The reason for this gradual change is PG&E's shifting revenue and cost structure (Figures 19 and 20). At higher levels of load defection, revenues from PG&E's wholesale generation and transmission businesses become more important, with transmission revenues becoming the utility's single largest revenue source. Both of these revenue streams benefit from higher overall demand in the CAISO system (i.e. hot years), which leads to a greater volume of electricity being distributed on PG&E's transmission facilities (a service for which even CCA customers in PG&E's territory pay, see Table 5). Despite the overall positive (and strengthening) relationship between annual demand and net revenues for PG&E, the very lowest net revenues actually occur in years when demand is moderate and wholesale prices are high. These years, which will be discussed next, are associated with drought and very low PG&E hydropower production.

Figure 24 shows the relationship between PG&E hydropower production (x-axis) and modeled annual net revenue (y-axis) under the three different load levels considered (current, 50% defection, 90% defection). Under current retail load levels, there is a strong positive correlation

between hydropower output at PG&E's dams and net revenue, with wet years being the most profitable. There are two reasons for this relationship. First, wet years result in greater production from PG&E's hydroelectric facilities, leading to higher revenues despite the lower wholesale prices.

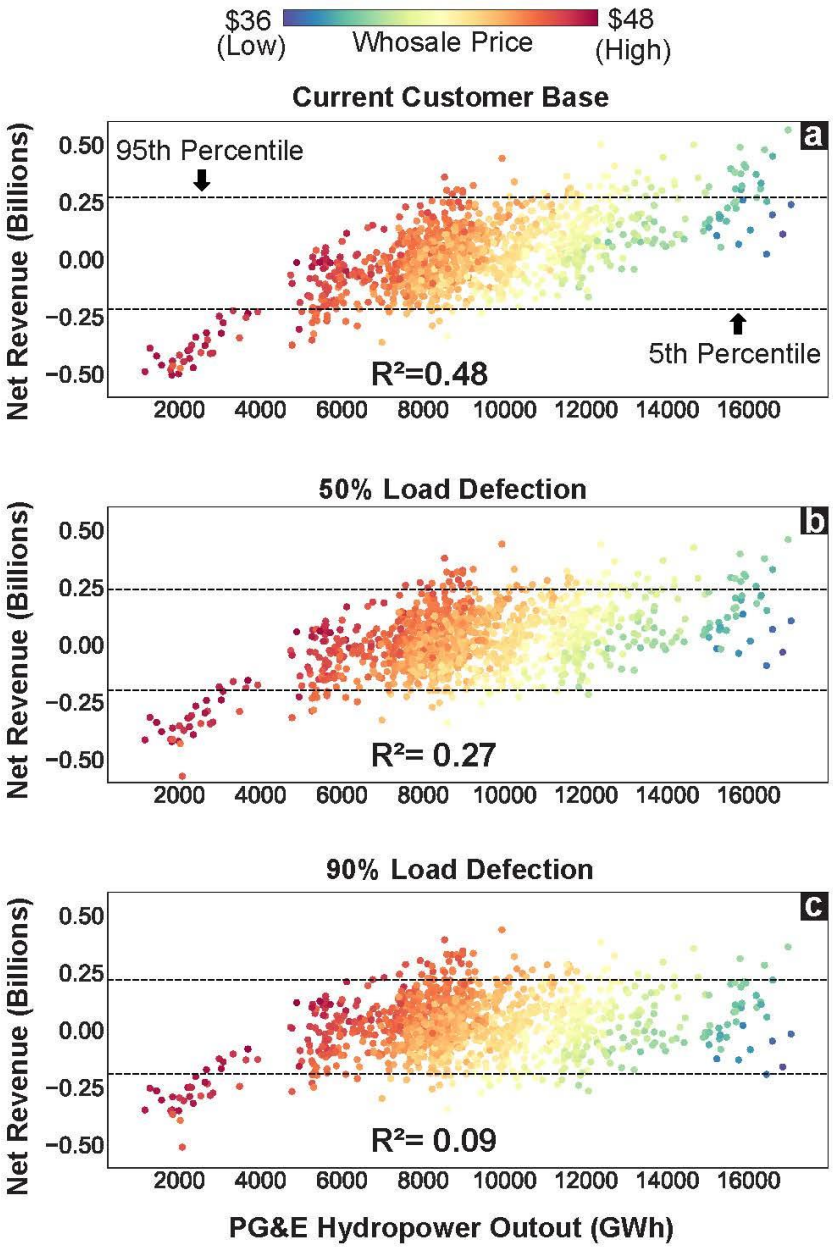

Figure 24: PG&E hydropower production and PG&E net revenues. The correlation between hydropower production and net revenues weakens as customers leave the system. Note that PG&E becomes financially exposed to extreme wet years at 90% load defection levels.

Second, wet years in California tend to experience lower wholesale electricity prices, due to a greater abundance of low marginal cost hydropower in the market. At current load levels, PG&E is usually a net buyer of electricity from the wholesale market, and lower prices during wet years would make it less expensive for the utility to meet its demand, increasing net revenues (this is also apparent in Figure 23a). Note however, that for any given level of hydropower production (take a vertical transect of Figure 24a), higher prices are generally better for net revenue. This actually reflects PG&E's exposure to air temperatures (hot years simultaneously increase market prices and increase demand in the PG&E footprint, which has a positive impact on net revenues).

The positive linear relationship between PG&E's hydropower production and its net revenues begins to break down as customers defect (Figure 24b and Figure 24c). While PG&E's negative financial exposure to very dry years remains steady, extremely high and low ($95^{th}/5^{th}$ percentile) net revenue years become associated with a much wider range of hydrologic conditions (this can also be seen Figures 23b and Figure 23c). As load leaves the system, even extremely wet years (historically a boon to PG&E and its fleet of hydroelectric dams) actually start to appear in the lower 5^{th} percentile of net revenue outcomes. These years are generally cooler years as well, experiencing low demand and thus contributing to very low market prices. As PG&E becomes a net seller into the CAISO market, these years of low demand (transmission revenues) and low wholesale prices become a liability.

As noted, a key element of PG&E's exposure to weather risk is not simply how temperature and streamflows affect demand and hydropower availability within the PG&E footprint, but also how these factors influence wholesale prices in the CAISO market. As PG&E experiences load defection, we see their exposure to wholesale price extremes change as well. Under current load levels, years of very high net revenues tend to concentrate around years of very low wholesale

prices (Figure 23a). Again, this is because of PG&E's current role as a net buyer of electricity; low prices make it cheaper to meet their retail demand. Low wholesale prices are also an indicator of high hydropower output, which is generally beneficial to PG&E. However, as PG&E experiences more load defection and transitions to a being a net seller in CAISO, their exposure to wholesale prices changes dramatically– nearly reversing (see Figures 23b and 23c). Another key to understanding this altered exposure is PG&E's reliance on long term PPAs for renewable energy, which were initiated as part of its efforts to comply with California's ambitious renewable energy portfolio standards. The reported average prices for these PPAs are around $140 per MW(Dudziak, Ewing and Horn, 2019) (a price that is typically much higher than the price in the CAISO market). As PG&E experiences load defection and transitions from a net buyer in the CAISO market to a net seller, PG&E is still contractually obligated by their PPAs. They continue to purchase renewable energy at a high price (re-selling it into CAISO for much less), a loss that becomes more damaging without the ability to pass these costs on to retail consumers. Consequently, very wet years that cause the market price to drop considerably) begin to represent a new liability for PG&E (Figures 23c and 24c).

4.4 CONCLUSION

Year-to-year fluctuations in streamflow and air temperatures are known to impact the operations of electricity markets like CAISO and financial outcomes of electricity utilities participating in those markets. Here, for the first time, we demonstrate that for one major utility, exposure to weather risk, including extremes, may change – and in a matter of years—not due to the effects of climate change, but due to retail load defection. As customers increasingly exert more control over the source of their electricity customer losses for incumbent utilities could disrupt their traditional business models, leading to changes in the relative importance of different cost and revenue components. These changes may significantly alter the very nature of a utility's

risk profile, including their exposure to weather.

In this study we use PG&E as a case study to demonstrate how its financial wellbeing is subject to uncertainty in two hydrometeorological variables, air temperatures and streamflow, which collectively influence electricity demand and hydropower output as well as wholesale prices in the CAISO market. We demonstrate how PG&E's exposure to uncertainty and extremes in each variable are likely to change as a function of retail load defection. Temperature will exhibit higher levels of correlation with net revenue. Streamflow's (hydropower output) relationship with net revenue remains the same during dry years, but wet years, which correlate with high net revenue years at current load levels, can even be harmful. This is caused by alteration in PG&E's business model from three aspects, 1) the relative weight of PG&E's revenue and cost sources will change; 2) PG&E transform from a net buyer into a net seller and 3) legal obligation to purchase renewable energy from the long term power purchase agreements.

There are a number of limitations in this work mostly related to a lack of detailed data about PG&E's business, including a lack of information about the exact structure of PG&E's active PPAs. In addition, we use a simplistic representation of PG&E electricity business, including a single rate structure for each customer class. We also assume that PG&E's fixed costs (O&M, debt service, etc.) are static, when in fact some year-to-year changes do occur (and may in the future as load defection increases). Lastly, we assume all load defection is caused by the formation of CCAs as opposed to DERs. This assumption is largely true based on historical data pattern. However, the implication of customer switching to DERs is different form load defect towards CCAs. The biggest difference is that CCA customers would still pay for transmission whereas DER owner do not and may even require PG&E to pay for their generation through net metering programs.

Nonetheless, the results of this work strongly suggest that utilities experiencing load

defection could experience altered exposure to weather risk. This could put additional pressure on utilities to rapidly adapt their risk management strategies. For PG&E in particular, this may represent an important challenge given its recent bankruptcy and precarious financial state. Although this work uses PG&E as a case study, other utilities that face load defection may experience similarly large alterations in their weather risk exposure, depending on their underlying generation portfolio, reliance on third party contracts, and the underlying causes of load defection.

REFERENCES

Bain, D. and Acker, T. (2018) 'Hydropower Impacts on Electrical System Production Costs in the Southwest United States', Energies, 11(2), p. 368. doi: 10.3390/en11020368.

Bartos, M. et al. (2016) 'Impacts of rising air temperatures on electric transmission ampacity and peak electricity load in the United States', Environmental Research Letters. IOP Publishing, 11(11). doi: 10.1088/1748-9326/11/11/114008.

BlackRock (2019) 'Getting physical: Scenario analysis for assessing climate-related risks', Global Insights, (April), pp. 1–20. doi: 10.1038/491S50a.

Bryant, S. T., Straker, K. and Wrigley, C. (2018) 'The typologies of power: Energy utility business models in an increasingly renewable sector', Journal of Cleaner Production. Elsevier Ltd, 195, pp. 1032–1046. doi: 10.1016/j.jclepro.2018.05.233.

California Public Utilites Commission (2020) Generate Rate Case. Available at: https://www.cpuc.ca.gov/General.aspx?id=10431.

Castaneda, M. et al. (2017) 'Myths and facts of the utility death spiral', Energy Policy. Elsevier Ltd, 110(June), pp. 105–116. doi: 10.1016/j.enpol.2017.07.063.

Collins, S. et al. (2018) 'Impacts of Inter-annual Wind and Solar Variations on the European Power System', Joule, 2(10), pp. 2076–2090.

Deng, S. (1999) 'Financial Methods in Competitive Electricity Markets', p. 139. Available at: http://www.ieor.berkeley.edu/~oren/students/shijie-d.pdf.

Deng, S. J. and Oren, S. S. (2006) 'Electricity derivatives and risk management', Energy, 31(6–7), pp. 940–953. doi: 10.1016/j.energy.2005.02.015.

Deng, T. et al. (2020) 'Risk evaluation and retail electricity pricing using downside risk constraints method', Energy. Elsevier Ltd, 192, p. 116672. doi: 10.1016/j.energy.2019.116672.

Denholm, P. et al. (2015) Overgeneration from Solar Energy in California. A Field Guide to the Duck Chart. Golden, CO (United States). doi: 10.2172/1226167.

Dudziak, R., Ewing, W. P. and Horn, J. E. Van (2019) 'Potential PG&E Bankruptcy Puts Power Purchase Agreement Counterparties On Notice'. Available at: https://btlaw.com/insights/alerts/2019/potential-pge-bankruptcy-puts-power-purchase-agreement-counterparties-on-notice.

Foster, B., Kern, J. and Characklis, G. (2015) 'Mitigating Hydrologic Financial Risk in Hydropower Generation Using Index-based Financial Instruments', Water Resources and Economics, 10, pp. 45–67.

Franco, G. and Sanstad, A. H. (2007) 'Climate change and electricity demand in California',

Climatic Change. doi: 10.1007/s10584-007-9364-y.

Gunther, S. J. and Bernell, D. (2019) 'Challenging the system: The role of community choice aggregation in California's transition to a renewable energy future', Electricity Journal. Elsevier, 32(10), p. 106679. doi: 10.1016/j.tej.2019.106679.

JOHN, J. ST. (2017) 'As California Mulls Retail Electricity Choice, Utilities Are Losing Customers in Droves', GreenTech Media. Available at: https://www.greentechmedia.com/articles/read/california-utilities-are-losing-customers-in-droves.

Kennedy, S. F. and Rosen, B. (2020) 'The rise of community choice aggregation and its implications for California's energy transition: A preliminary assessment', Energy and Environment. doi: 10.1177/0958305X20927381.

Kern, J. and Characklis, G. (2017) 'Evaluating the Financial Vulnerability of a Major Electric Utility in the Southeastern U.S. to Drought under Climate Uncertainty and an Evolving Generation Mix', Environmental Science and Technology, 55(15), pp. 8815–8823.

Kern, J. D., Characklis, G. W. and Foster, B. T. (2015) 'Natural gas price uncertainty and the cost-effectiveness of hedging against low hydropower revenues caused by drought', Water Resources Research, 51(4), pp. 2412–2427. doi: 10.1002/2014WR016533.

Kern, J. D., Su, Y. and Hill, J. (2020) 'A retrospective study of the 2012-2016 California drought and its impacts on the power sector', Environmental Research Letters. Available at: http://iopscience.iop.org/10.1088/1748-9326/ab9db1.

Kraft, B. (2018) 'Shedding Light on Stakeholder Power in a Regulated Market: A Study of Variation in Electric Utilities' Climate Change Disclosures', Organization and Environment, 31(4), pp. 314–338. doi: 10.1177/1086026617718429.

Laws, N. D. et al. (2017) 'On the utility death spiral and the impact of utility rate structures on the adoption of residential solar photovoltaics and energy storage', Applied Energy. Elsevier Ltd, 185, pp. 627–641. doi: 10.1016/j.apenergy.2016.10.123.

Mazdiyasni, O. and AghaKouchak, A. (2015) 'Substantial increase in concurrent droughts and heatwaves in the United States', Proceedings of the National Academy of Sciences, 112(37), pp. 11484–11489. doi: 10.1073/pnas.1422945112.

McKinsey Global Institute (2020) Climate Risk and response.

Mureddu, M. and Meyer-Ortmanns, H. (2018) 'Extreme prices in electricity balancing markets from an approach of statistical physics', Physica A: Statistical Mechanics and its Applications. Elsevier B.V., 490, pp. 1324–1334. doi: 10.1016/j.physa.2017.09.001.

Nierop, S. C. A. (2014) 'Envisioning resilient electrical infrastructure: A policy framework for incorporating future climate change into electricity sector planning', Environmental Science and Policy. Elsevier Ltd, 40, pp. 78–84. doi: 10.1016/j.envsci.2014.04.011.

O'Shaughnessy, E. et al. (2019) 'Community Choice Aggregation- Challenges, Opportunities, and Impacts on Renewable Energy Markets', (February).

Pacific Gas and Electric Company (2017) 'Pacific Gas and Electric Company 2017 Joint Annual Report to Shareholders'.

Pacific Gas and Electric Company (2019) 'Pacific Gas and Electric Company 2019 Joint Annual Report to Shareholders'.

Pappas, S. S. et al. (2008) 'Electricity demand loads modeling using AutoRegressive Moving Average (ARMA) models', 33, pp. 1353–1360. doi: 10.1016/j.energy.2008.05.008.

Sautter, J. A. and Twaite, K. (2009) 'A Fractured Climate? The Political Economy of Public Utility Commissions in an Age of Climate Change', Electricity Journal, 22(6), pp. 68–76. doi: 10.1016/j.tej.2009.05.010.

Su, Y. et al. (2019) 'An open source model for quantifying risks in bulk electric power systems from spatially and temporally correlated hydrometerological processes', Environmental Modelling and Software.

Su, Y., Kern, Jordan D., et al. (2020) 'An open source model for quantifying risks in bulk electric power systems from spatially and temporally correlated hydrometeorological processes', Environmental Modelling and Software. Elsevier Ltd, 126. doi: 10.1016/j.envsoft.2020.104667.

Su, Y., Kern, Jordan D, et al. (2020) 'Compound hydrometeorological extremes across multiple timescales drive volatility in California electricity market prices and emissions', Applied Energy. Elsevier, 276(April), p. 115541. doi: 10.1016/j.apenergy.2020.115541.

Su, Y., Kern, J. D. and Characklis, G. W. (2017) 'The impact of wind power growth and hydrological uncertainty on financial losses from oversupply events in hydropower-dominated systems', Applied Energy, 194. doi: 10.1016/j.apenergy.2017.02.067.

Taminiau, J. et al. (2019) 'Advancing transformative sustainability: A comparative analysis of electricity service and supply innovators in the United States', Wiley Interdisciplinary Reviews: Energy and Environment, 8(4), pp. 1–16. doi: 10.1002/wene.337.

CHAPTER 5: CONCLUSIONS AND FUTURE WORK

Hydrometerological variability can have significant impacts on power systems' operations by impacting both the supply of and demand for electricity. Hydrologic conditions, wind speeds and irradiance directly impact the availability of hydropower, wind power and solar power, respectively. On the demand side, air temperatures strongly influence electricity consumption for heating and cooling needs. Large fluctuations in these hydrometeorological forcings can influence wholesale electricity prices, GHG emissions and even system reliability across multiple time scales. This work evaluates risk for the electricity sector and specific system participants resulting from fluctuations in spatially and temporally correlated hydrometerological conditions, focusing on California and the U.S. West Coast.

In California, air temperatures and hydrologic conditions are the main environmental drivers of wholesale market prices on an annual level. However, zooming in from annual to daily and hourly time steps, the effects of variable renewable energy (wind and solar) on extreme power prices becomes more important. Extreme low prices on both a daily and hourly time scale are routinely caused by a combination of low demand and an abundance of renewable energy. Extreme high price daily events are likely to occur in mid to late August due to the reduced hydropower capacity (diminishing post snowmelt streamflow conditions) and a high potential for heat waves. On an hourly basis, extreme high price events are likely to occur around sunset, when the system struggles to replace rapidly diminishing solar power.

The risks and uncertainties in the West Coast bulk power system and wholesale electricity

markets are experienced uniquely by different system participants and can interact with others sources of risk as well. In California in particular, competition in retail electricity markets is profoundly impacting incumbent utilities— drastically reducing revenues from utilities' retail businesses and in the process, altering utilities' exposure to weather risk. Using Pacific Gas and Electric (PG&E) as an example, load defection makes the utility's transmission revenue more important, which in turn make's PG&E's financial performance more contingent on system-wide demand. As a result, air temperatures become a better proxy for variability in PG&E's net revenues on an annual basis. At the same time, load defection changes PG&E's financial exposure to hydrologic conditions. Dry years remain harmful, however, very wet years (associated with an overabundance of hydropower and low wholesale prices) also become a source of risk as PG&E becomes a "net seller" into the wholesale market.

This work clearly illustrates that significant risks are caused by hydrometerological uncertainty and extremes, and goes further to rigorously quantify these risks. Moving forward, there are many other sources of uncertainty that warrant further investigation in the power system sector. Relative to this analysis which focused largely on stationary hydrometerological uncertainties, climate change is one of the biggest outstanding questions for power systems participants. Climate change is altering average weather conditions and, perhaps just as importantly, exacerbating the magnitude of some extreme events, leading to potentially much more severe consequences for power system participants.

In addition, the underlying generation mix is also changing. For example, the West Coast power system has already witnessed rapid increases in renewable penetration in the last few years and this trend is likely to continue. Even more substantial changes are expected in the coming 5-10 years, most notably the addition of battery storage in the system, more renewable energy and

the retirement of fossil fuel-based generation assets. On the demand side, the historically well-defined demand pattern is likely to evolve due to the electrification of the transportation sector. These are all changes that are likely to interact in complex ways with weather uncertainty.

This work also explores the effect that changes in regulation and market structure can have on utility's financial risk exposure, but there are a number of other regulations and policies that can affect utilities' business models and investment in infrastructure. These must also be explored.

Future research should seek to address the potential for these sources of uncertainty to impact the power sector individually and in combination. Given the diversity of market settings, regulatory institutions and underlying generation mixes that exist across regions and countries, dedicated research for each market/region may be required in some cases.

Uncertainty characterization is not the end goal. Risk management strategies need to be developed to deal with the uncertainties uncovered in the system. Future research in this area should use improved characterization of risks to design and implement optimal portfolios of hedging strategies that can be adapted as exposure changes. For example, results from Chapter 4 suggest that maintaining the same weather-based hedging strategies as utilities lose retail customers will not be effective, and could even become harmful to the utilities' financial well-being. Hedging strategies must be adapted (perhaps on an annual basis) as weather exposure changes due to retail load defection. One approach would be a Multi-Objective Direct Policy Search framework. This method would use an evolutionary algorithm to search for optimal hedging policies, which could include a combination of heating and cooling degree day contracts, snowpack index insurance, the use of a contingency fund, debt, and power price derivatives. Better management of risks is in turn likely to facilitate better infrastructure investment decisions.

While the focus of this work is primarily on the West Coast grid, specifically California

and PG&E, some lessons from this research easily extend to other electricity systems and utilities in the U.S., as well as globally. The same fundamental weather risks (impacts on supply and demand) exist elsewhere, which ultimately translate to dynamically changing prices and greenhouse gas emissions. The deregulation of retail markets, which is also happening elsewhere in the U.S. and the rest of the world, is widely expected to change the existing business model for the incumbent utilities. The insights and knowledge gained from California utilities can be applied to other utilities in different settings.

Significant changes in power sector are expected to come in the next few decades. A better understanding of how weather risk with interact with these changes, both from a system operator's perspective and individual participant's perspective, can facilitate better decision making related to long-term capital investment and short-term operations. In turn, better-managed electricity systems will significantly improve the efficiency of decarbonization efforts to combat climate change.